Synthesis, Structure, and Ligand Dynamics of Triosmium Imidoyl Clusters and Their Isocyanide Derivatives

Michael Day, David Espitia, Kenneth I. Hardcastle, Shariff E. Kabir, Tim McPhillips, and Edward Rosenberg*

California State University, Northridge, California 91330

Roberto Gobetto, Luciano Milone,* and Domenico Osella

Dipartimento di Chimica Inorganica, Chimica Fisica e Chimica dei Materiali, Università di Torino, Via Giuria 7-9, Torino, Italy I 10125

Received November 25, 1992

The synthesis of $(\mu\text{-H})(\mu\text{-}\eta^2\text{-}\overline{C{=}NCH_2CH_2CH_2})Os_3(CO)_{10}$ (**10**), the coproduct $(\mu\text{-H})(\mu\text{-}\eta^1\text{-}\overline{NCH_2CH_2CH_2CH_2})Os_3(CO)_{10}$ (**9**) and the related imidoyl cluster $(\mu\text{-H})(\mu\text{-}\eta^2\text{-}CH_3CH_2C{=}NCH_2CH_2CH_3)Os_3(CO)_{10}$ (**11**) are reported. Thermolysis of **9** at 98 °C yields **10** quantitatively, and both **10** and **11** are decarbonylated thermally or photochemically to yield μ_3-imidoyl clusters $(\mu\text{-H})(\mu_3\text{-}\eta^2\text{-}\overline{C{=}NCH_2CH_2CH_2})Os_3(CO)_9$ (**2**) and $(\mu\text{-H})(\mu_3\text{-}\eta^2\text{-}CH_3CH_2C{=}NCH_2CH_2CH_3)Os_3(CO)_9$ (**3**), respectively. The reactions of **2** and **3** with RNC (R = CH_3, $C(CH_3)_3$) are reported, and in both cases initial adducts $(\mu\text{-H})(\mu\text{-}\eta^2\text{-}\overline{C{=}NCH_2CH_2CH_2})Os_3(CO)_9(CNR)$ (R = CH_3, **12**; R = $C(CH_3)_3$, **13**) and $(\mu\text{-H})(\mu\text{-}\eta^2\text{-}CH_3CH_2C{=}NCH_2CH_2CH_3)Os_3(CO)_9(CNR)$ (R = CH_3, **14**; R = $C(CH_3)_3$, **15**) are isolated in high yield. Thermolysis of **12–15** at 128 °C yields the μ_3-imidoyl complexes $(\mu\text{-H})(\mu_3\text{-}\eta^2\text{-}\overline{C{=}NCH_2CH_2CH})_2Os_3(CO)_8(CNR)$ (R = CH_3, **16**; R = $C(CH_3)_3$, **17**) and $(\mu\text{-H})(\mu_3\text{-}\eta^2\text{-}CH_3CH_2C{=}NCH_2CH_2CH_3)Os_3(CO)_8(CNR)$ (R = CH_3, **18**; R = $C(CH_3)_3$, **19**). Variable temperature ^{1}H- and ^{13}C-NMR and ^{1}H- and ^{13}C-EXSY experiments are reported for **2**, **10**, and **16-19** which reveal, in detail, the multistage nature of the ligand exchange processes. In solution, complexes **12-19** exist as a large number of positional isomers which do not interconvert in the case of **12-15** but which are interconverted by the motion of the μ_3-imidoyl ligand and axial–radial exchange in **16-19**. Solid-state structures for **2**, **9**, **12**, **13**, and **16** are reported. Compound **2** crystallizes in the monoclinic space group $P2_1/m$ with unit cell parameters a = 7.681(1) Å, b = 14.801(2) Å, c = 8.157(2) Å, β = 106.06(1)°, V = 891(1) Å^3, and Z = 2. Least-squares refinement of 2179 reflections gave a final agreement factor of R = 0.044 (R_w = 0.043). Compound **9** crystallizes in the triclinic space group $P2_1$ with unit cell parameters a = 9.294(3) Å, b = 15.758(5) Å, c = 7.406(2) Å, α = 81.10(2)°, β = 76.47(2)°, γ = 74.88(2)°, V = 992(1) Å^3, and Z = 2. Least-squares refinement of 2677 reflections gave a final agreement factor of R = 0.037 (R_w = 0.044). Compound **12** crystallizes in the monoclinic space group $P2_1/n$ with unit cell parameters a = 8.987(2) Å, b = 16.067(2) Å, c = 14.436(3) Å, β = 93.06(1)°, V = 2081(1) Å^3, and Z = 4. Least-squares refinement of 2579 reflections gave a final agreement factor of R = 0.051 (R_w = 0.057). Compound **13** crystallizes in the monoclinic space group $P2_1/c$ with unit cell parameters a = 9.216(1) Å, b = 19.372(5) Å, c = 15.176(3) Å, β = 116.38(2)°, V = 2427(2) Å^3, and Z = 4. Least-squares refinement of 4673 reflections gave a final agreement factor of R = 0.044 (R_w = 0.053). Compound **16** crystallizes in the triclinic space group $P2_1/c$ with unit cell parameters a = 8.574(4) Å, b = 15.660(6) Å, c = 8.437(2) Å, α = 80.69(4)°, β = 67.12(4)°, γ = 74.09(4)°, V = 1002(1) Å^3, and Z = 2. Least-squares refinement of 3738 reflections gave a final agreement factor of R = 0.058 (R_w = 0.061).

Introduction

We recently reported, in preliminary form,[1] room temperature, selective, α-carbon–hydrogen bond activation in the reactions of pyrrolidine and di-*n*-propylamine with $Os_3(CO)_{10}(CH_3CN)_2$ (**1**). The resulting μ_3-imidoyl complexes **2** and **3**, obtained after decarbonylation of the initial products (eqs 1 and 2), exhibited an unusually low barrier to the co-called "windshield wiper" motion of the organic ligand over the face of the metal cluster (Scheme I) relative to other μ_3 five electron donor ligands.[1] We subsequently found that this higher degree of fluxionality is associated with a higher reactivity toward addition of a range of phosphine donor ligands and that the structure of the resulting addition products (**4–6**) is sensitive to the steric bulk of the phosphine ligand as well as to the structure

Scheme I

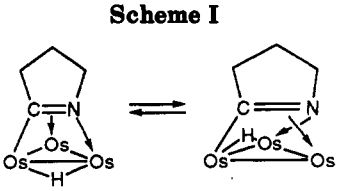

(1) Rosenberg, E.; Kabir, S. E.; Hardcastle, K. I.; Day, M.; Wolf, E. *Organometallics* **1990**, *9*, 2214.

0276-7333/93/2312-2309$04.00/0

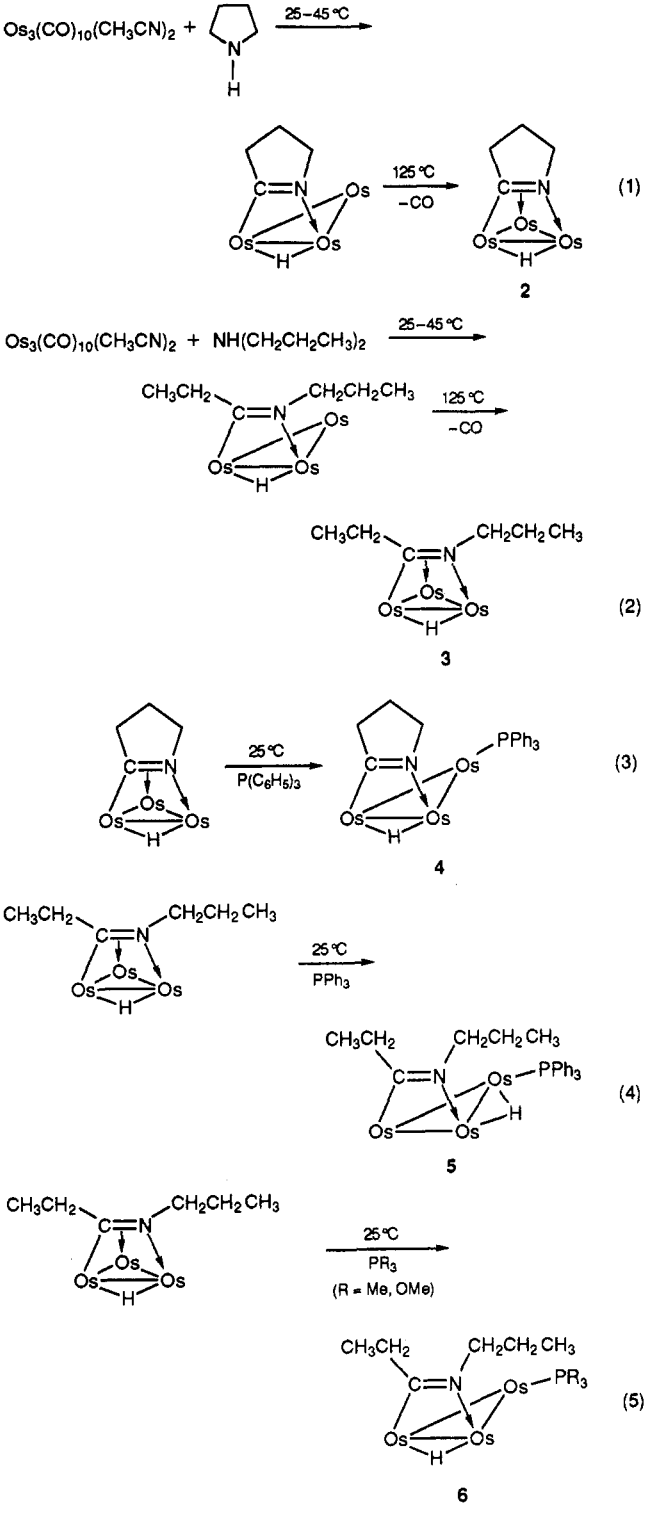

(1) (2) (3) (4) (5)

of the imidoyl ligand[2] (eqs 3–5). Thermolysis of the phosphine adducts **4** and **5** leads to isomerization and then decarbonylation to give isostructural phosphine substituted derivatives of **2** and **3** (eqs 6 and 7, compounds **7** and **8**) in which the imidoyl ligand is static on the NMR time scale up to +80 °C.[2] In order to investigate the relationship of the added two electron-donor ligand toward the structure of the addition products, the barriers to the structure of the addition products, the barriers to the subsequent isomerizations, and the barrier to the windshield wiper motion of the imidoyl ligand, we undertook a study of the reactions of **2** and **3** with methyl and *tert*-butyl isocyanide. We report here the results of these studies where, although we observe the same overall reactivity as with phosphines, we see a marked difference in the structures, the barriers toward isomerizations, and ligand migrations of the products obtained. We also report the full details of the synthesis of **2** and **3** and the structure of **2** and of the coproduct (μ-H)(μ-η^1-NCH$_2$CH$_2$CH$_2$CH$_2$)-Os$_3$(CO)$_{10}$ (**9**), as well as the 2D-^{1}H- and ^{13}C-EXSY studies of **2**, its precursor, (μ-H)Os$_3$(CO)$_{10}$(μ-η^2-C=NCH$_2$CH$_2$CH$_2$), and its isocyanide derivatives.

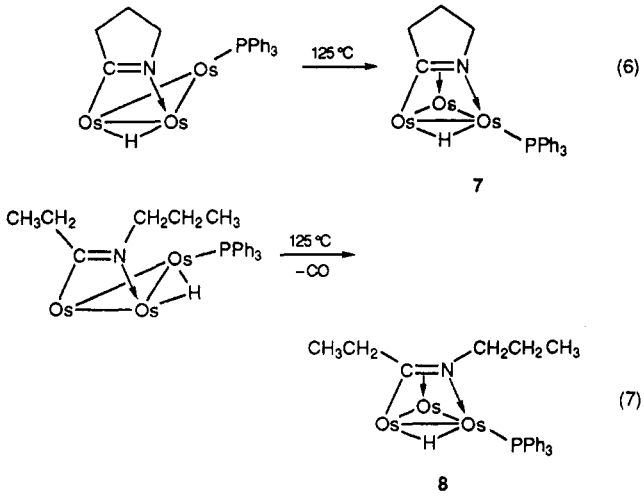

(6) (7)

Results and Discussion

A. Synthesis of 2 and 3 and Structures of 2 and 9. The reaction of pyrrolidine with **1** in benzene at 40–45 °C for 8 h yields the μ-imidoyl complex (μ-H)(μ-η^2-C=NCH$_2$CH$_2$CH$_2$CH$_2$)Os$_3$(CO)$_{10}$ (**10**) in 50% yield (eq 1). In addition, (μ-H)(μ-η^1-NCH$_2$CH$_2$CH$_2$CH$_2$)Os$_3$(CO)$_{10}$ (**9**) is obtained in 7% yield as well as (μ-H)$_2$Os$_3$(CO)$_{10}$[3] (4%). At room temperature in methylene chloride for 24 h the same overall reaction is observed but somewhat lower yields of **10** are obtained (15–20%). If preparations of **1** containing small amounts of Os$_3$(CO)$_{11}$(CH$_3$CN) are used, the complex (μ-H)(μ-η^2-O=CNCH$_2$CH$_2$CH$_2$CH$_2$)Os$_3$(CO)$_{10}$ is also obtained.[1] This is verified by separate reactions of pyrrolidine with Os$_3$(CO)$_{11}$(CH$_3$CN) where the carbamoyl complex is the only product obtained and demonstrates that a binuclear site must be available to the secondary amine in order to form the imidoyl complex **10**.

Thermolysis of **9** in heptane for 4 h at 98 °C yields **10** quantitatively but no conversion of **9** to **10** is observed at 20–45 °C in benzene or methylene chloride using the reaction times noted above (eq 8). This result indicates

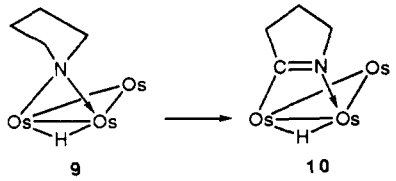

(8)

that **9** is not a direct precursor to **10** under the reaction

(2) Day, M.; Espitia, D.; Hardcastle, K. I.; Kabir, S. E.; Rosenberg, E.; Gobetto, R.; Milone, L.; Osella, D. *Organometallics* **1991**, *10*, 3550.

(3) (a) Knox, S. A. R.; Koepke, J. W.; Andrews, M. A.; Kaesz, H. D. *J. Am. Chem. Soc.* **1975**, *97*, 2942. (b) Sappa, E.; Valle, M. *Inorg. Synth.* **1989**, *26*, 365.

Table I. Crystal Data Collection and Refinement Parameters

	2	9	12	13	16
formula	$C_{13}H_7NO_9Os_3$	$C_{14}H_9NO_{10}Os_3$	$C_{15}H_{10}N_2O_9Os_3$	$C_{18}H_{16}N_2O_9Os_3$	$C_{14}H_{10}N_2O_8Os_3$
fw	891.80	921.83	932.85	974.94	904.84
cryst syst	monoclinic	monoclinic	monoclinic	monoclinic	triclinic
space group	$P2_1/m$	$P2_1$	$P2_1/n$	$P2_1/c$	$P\bar{1}$
a, Å	7.681(1)	9.164(1)	8.987(2)	9.216(1)	8.574(4)
b, Å	14.801(2)	8.696(1)	16.067(3)	19.372(5)	15.660(6)
c, Å	8.157(2)	12.678(1)	14.436(3)	15.176(3)	8.437(2)
α, deg					80.69(4)
β, deg	106.06(1)	101.02(2)	93.06(1)	116.38(2)	67.12(4)
γ, deg					74.09(4)
V, Å^3	891(1)	992(1)	2081(1)	2427(2)	1002(1)
Z	2	2	4	4	2
D_{calc}, g/cm^3	3.32	3.09	2.98	2.67	3.00
abs coeff (μ), cm^{-1}	214.2	192.5	183.4	157.37	190.5
data collect temp, °C	25 ± 1	25 ± 1	25 ± 1	25 ± 1	25 ± 1
radiation	Mo Kα	Mo Kα	Mo Kα	Mo Kα	Mo Kα
scan mode	ω–2θ	ω–2θ	ω–2θ	ω–2θ	ω–2θ
scan limits, deg	$2 < 2\theta < 68$	$2 < 2\theta < 56$	$2 < 2\theta < 48$	$2 < 2\theta < 56$	$2 < 2\theta < 60$
scan speed, deg/min	8.2	1.7–8.2	7.2–8.2	5.5	8.2
scan range, deg	0.8	0.9	0.8	1.0	1.0
no. of data collcd	3744	4777	3398	6030	5817
no. of data obsd	2179	4403	2579	4673	3738
no. of variables	124	252	262	289	244
R^a	0.044	0.037	0.051	0.044	0.058
R_w^b	0.043	0.044	0.057	0.053	0.061
largest shift/esd	0.05	0.01	0.01	0.03	0.01
weighting scheme	$1/\sigma^2$	$1/\sigma^2$	$1/\sigma^2$	$1/\sigma^2$	$1/\sigma^2$
highest peak in final diff map, e/Å^3	1.91 (41)	4.14 (41)	2.03 (32)	2.79 (38)	2.58 (39)
rel transm coeff	0.42–1.00	0.24–1.00	0.53–1.00	0.49–1.00	0.38–0.99

^{a} $R = \Sigma(|F_o| - |F_c|)/\Sigma|F_o|$. ^{b} $R_w = [(\Sigma w(|F_o| - |F_c|)^2/\Sigma w|F_o|^2]^{1/2}$.

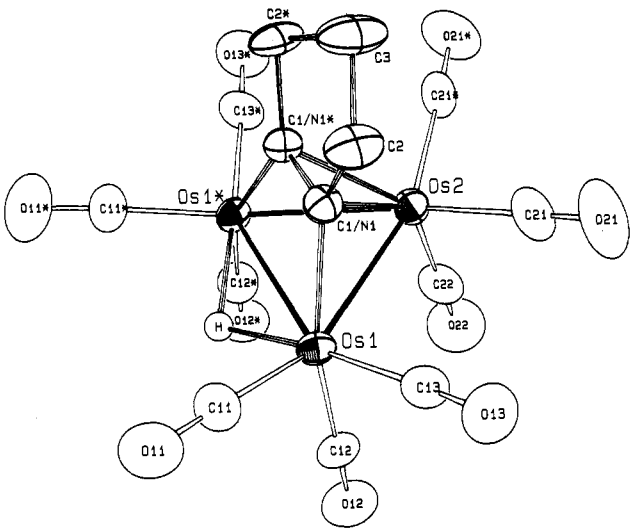

Figure 1. ORTEP drawing of (μ-H)(μ_3-η^2-C=NCH$_2$CH$_2$CH$_2$)Os$_3$(CO)$_9$ (**2**) showing the calculated position of the hydride. Atoms marked with an asterisk are interchangeable since the molecule lies on a crystallographic mirror plane.

conditions where **10** is formed as the major product and makes the important point that aliphatic α-carbon–hydrogen bond activation is competitive with nitrogen–hydrogen bond activation at binuclear metal sites. Compound **10** slowly decarbonylates to the μ_3-imidoyl complex **2** in refluxing octane (128 °C) (eq 1). Although yields of **2** by this method can approach 90%, the inordinately long reaction times (~24 h) prompted us to attempt this decarbonylation photochemically. Indeed, irradiating **10** at 3000 Å for 1.5 h gives **2** in 90% yield.

We previously reported the structure of **10** and report here, for comparison with other μ_3-imidoyl complexes,[4] the structure of **2**. The structure of **2** is shown in Figure 1, crystal data are in Table I, atomic coordinates are in Table II and selected distances and bond angles are in Table III. The structure of complex **2** is disordered with respect to the metal-bound carbon and nitrogen atoms because the μ_3-imidoyl ligand sits on a crystallographic mirror plane. Compound **2** has an isosceles triangle of osmium atoms (Os1–Os2 = Os1*–Os2 = 2.744(1) Å) with one elongated metal–metal edge (Os1–Os1* = 3.010(1) Å) where the hydride ligand is undoubtedly located. The location of the hydride (Figure 1) was calculated using the potential energy minimum program Hydex[5] and is estimated to lie 0.36 Å below the Os$_3$ plane essentially *trans* to CO13 and CO13*. Compound **2** crystallizes in the same

Table II. Fractional Atomic Coordinates for (μ-H)(μ_3-η^2-C=NCH$_2$CH$_2$CH$_2$)Os$_3$(CO)$_9$ (2)

atom	x	y	z	B (Å^2)^a
Os1	0.23065(6)	0.35166(3)	–0.16359(5)	2.157(8)
Os2	0.12915(9)	0.250	0.07592(8)	2.34(1)
O11	0.484(1)	0.4226(9)	–0.364(1)	5.8(3)
O12	–0.125(1)	0.3918(8)	–0.428(1)	5.0(3)
O13	0.221(1)	0.5292(7)	0.017(1)	5.3(3)
O21	0.106(2)	0.4028(8)	0.318(1)	7.5(3)
O22	–0.267(2)	0.250	–0.130(2)	6.3(5)
C1/N1	0.402(1)	0.2956(7)	0.056(1)	2.3(2)
C2	0.546(2)	0.334(1)	0.205(1)	3.3(3)
C3	0.587(3)	0.250	0.324(2)	4.4(5)
C11	0.392(2)	0.396(1)	–0.283(2)	3.5(3)
C12	0.008(2)	0.379(1)	–0.331(1)	3.1(3)
C13	0.223(2)	0.4635(9)	–0.046(1)	3.5(3)
C21	0.112(2)	0.348(1)	0.232(1)	4.1(3)
C22	–0.122(3)	0.250	–0.054(2)	4.1(5)
H	0.228	0.250	–0.296	6.0*

^{a} The starred value refers to the atom that was refined isotropically. Anisotropically refined atoms are given in the form of the isotropic equivalent displacement parameter defined as $(4/3)[a^2B(1,1) + b^2B(2,2) + c^2B(3,3) + ab(\cos\gamma)B(1,2) + ac(\cos\beta)B(1,3) + bc(\cos\alpha)B(2,3)]$.

(4) Day, M.; Hajela, S.; Kabir, S. E.; Irving, M.; McPhillips, T.; Wolf, E.; Hardcastle, K. I.; Rosenberg, E.; Gobetto, R.; Milone, L.; Osella, D. *Organometallics* **1991**, *10*, 2743.
(5) Orpen, A. G. *J. Chem. Soc., Dalton Trans.* **1980**, 2509.

Table III. Selected Bond Distances (Å) and Angles (deg) for $(\mu\text{-H})(\mu\text{-}\eta^2\text{-C}{=}\overline{\text{NCH}_2\text{CH}_2\text{CH}_2}\text{)Os}_3(\text{CO})_9$ (2)[a]

		Distances	
Os1–Os1*	3.010(1)	C1/N1–C1/N1*	1.35(2)
Os1–Os2	2.7441(7)	C1/N1–C2	1.51(1)
Os1–C1/N1	2.079(9)	C2–C3	1.55(2)
Os2–C1/N1	2.250(9)	Os–C(CO)	1.92(3)[b]
Os1–H	1.85	C–O(CO)	1.12(3)[b]
		Angles	
Os1*–Os1–Os2	56.75(1)	C1/N1*–C1/N1–C2	112.2(7)
Os1–Os2–Os1*	66.50(3)	C1/N1–C2–C3	100(1)
Os–C–O(CO)	178(2)	C2–C3–C2*	107(2)

[a] Numbers in parentheses are estimated standard deviations in the least significant digits. [b] Average values.

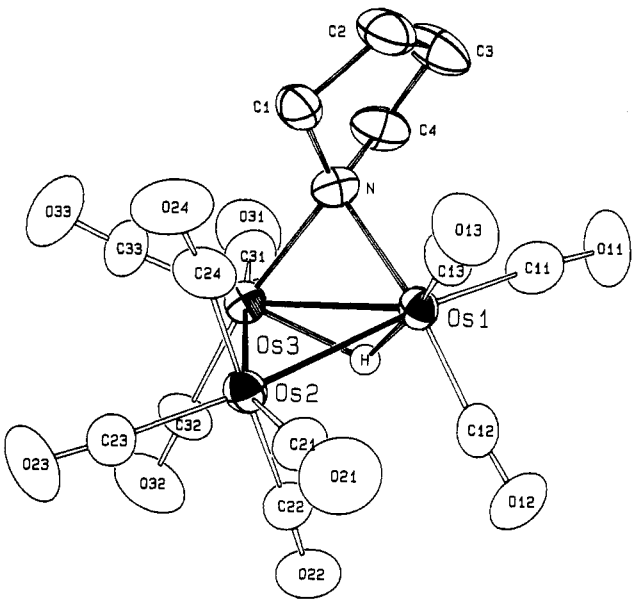

Figure 2. ORTEP drawing of $(\mu\text{-H})(\mu\text{-}\eta^1\text{-}\overline{\text{NCH}_2\text{CH}_2\text{CH}_2\text{CH}_2}\text{)-Os}_3(\text{CO})_{10}$ (9) showing the calculated position of the hydride ligand.

space group ($P2_1/m$) with the same unit cell parameters as the ruthenium analog,[4] and its structural geometry is virtually identical with the exception of minor variances in the bond distances. Compared with **10** significant changes occur in the metal–metal, metal–ligand, and ligand–ligand bonds.[7] The doubly bridged metal–metal edge lengthens by about 0.05 Å, and the unbridged metal–metal edges shorten by about 0.13 Å. These changes are undoubtedly associated with the formation of a π-bond to the rear metal atom. As expected, significant lengthening of the C1–N bond is observed in **2** compared with **10** (C1–N = 1.25(2) Å in **10**[1] and 1.30(2) Å in **2**).

Although direct analogs of **9** have been reported, specifically $(\mu\text{-H})(\eta^1\text{-NR}_2)\text{Os}_3(\text{CO})_{10}$ (R = CH_3)[6] and $(\mu\text{-H})(\mu\text{-}\eta^1\text{-N(H)R)Os}_3(\text{CO})_{10}$ (R = CH_3,[7] η-C_4H_9,[8] C_6H_5,[9] $CH_2C_6H_5$[9]), no solid-state structures of these μ-amido complexes have been reported to date. The solid-state structure of **9** is illustrated in Figure 2, crystal data are given in Table I, atomic coordinates are in Table IV, and

Table IV. Fractional Atomic Coordinates for $(\mu\text{-H})(\mu\text{-}\eta^1\text{-}\overline{\text{NCH}_2\text{CH}_2\text{CH}_2\text{CH}_2}\text{)Os}_3(\text{CO})_{10}$ (9)

atom	*x*	*y*	*z*	*B* (Å²)[a]
Os1	0.13886(4)	0.000	0.23707(3)	2.621(7)
Os2	0.42264(5)	–0.06603(6)	0.18468(3)	2.986(7)
Os3	0.22657(5)	–0.30595(6)	0.22262(3)	2.816(7)
O11	–0.175(1)	0.085(2)	0.263(1)	6.5(3)
O12	0.087(1)	0.212(1)	0.0433(9)	6.1(3)
O13	0.293(1)	0.254(1)	0.375(1)	6.3(3)
O21	0.512(2)	0.265(1)	0.150(1)	8.1(3)
O22	0.243(1)	–0.083(2)	–0.0472(8)	5.8(3)
O23	0.680(1)	–0.250(2)	0.126(1)	7.4(3)
O24	0.607(1)	–0.064(2)	0.412(1)	7.7(4)
O31	0.004(1)	–0.563(1)	0.238(1)	5.6(2)
O32	0.267(2)	–0.447(2)	0.011(1)	7.6(3)
O33	0.495(1)	–0.468(2)	0.347(1)	6.8(3)
N	0.174(1)	–0.178(1)	0.3556(7)	3.1(2)
C1	0.281(1)	–0.161(2)	0.461(1)	3.9(3)
C2	0.179(2)	–0.088(2)	0.535(1)	5.0(3)
C3	0.025(1)	–0.135(2)	0.489(1)	5.1(3)
C4	0.038(1)	–0.236(2)	0.3939(9)	3.9(2)
C11	–0.060(1)	0.045(2)	0.256(1)	4.0(3)
C12	0.110(1)	0.129(2)	0.114(1)	4.0(3)
C13	0.235(1)	0.159(1)	0.325(1)	3.7(2)
C21	0.486(1)	0.139(2)	0.164(1)	4.0(3)
C22	0.304(2)	–0.076(2)	0.039(1)	4.2(3)
C23	0.585(2)	–0.181(2)	0.145(1)	5.1(3)
C24	0.528(1)	–0.065(2)	0.329(1)	4.3(2)
C31	0.084(2)	–0.464(1)	0.234(1)	3.9(3)
C32	0.254(2)	–0.391(2)	0.090(1)	4.8(3)
C33	0.394(2)	–0.408(2)	0.297(1)	4.2(3)
H	0.083	–0.171	0.152	4.0*

[a] The starred value refers to the atom that was anisotropically refined atoms are given in the form of the isotropic equivalent displacement parameter defined as $(4/3)[a^2B(1,1) + b^2B(2,2) + c^2B(3,3) + ab(\cos\gamma)B(1,2) + ac(\cos\beta)B(1,3) + bc(\cos\alpha)B(2,3)]$.

Table V. Selected Bond Distances (Å) and Angles (deg) for $(\mu\text{-H})(\mu\text{-}\eta^1\text{-}\overline{\text{NCH}_2\text{CH}_2\text{CH}_2\text{CH}_2}\text{)Os}_3(\text{CO})_{10}$ (9)[a]

		Distances	
Os1–Os2	2.8625(6)	N–C1	1.50(1)
Os1–Os3	2.7953(5)	C1–C2	1.58(2)
Os2–Os3	2.8535(7)	C2–C3	1.48(2)
Os1–H	1.85	C3–C4	1.52(2)
Os3–H	1.85	N–C4	1.51(2)
Os1–N	2.141(9)	Os–C(CO)	1.91(3)[b]
Os3–N	2.15(1)	C–O(CO)	1.14(2)[b]
		Angles	
Os1–Os2–Os3	58.55(1)	C1–N–C4	100.7(9)
Os1–Os3–Os2	60.88(2)	N–C1–C2	102(1)
Os2–Os1–Os3	60.56(2)	C1–C2–C3	107(1)
Os–C–O(CO)	176(2)[b]	C2–C3–C4	105(1)
		N–C4–C3	105(1)

[a] Numbers in parentheses are estimated standard deviations in the least significant digits. [b] Average values.

selected distances and bond angles are in Table V. Compound **9** exists as an approximate isosceles triangle of osmium atoms (Os1–Os2 = 2.863(1) Å, Os2–Os3 = 2.854(1) Å, and Os1–Os3 = 2.795(1) Å), with the organic ligand and the hydride bridging the shortened Os1–Os2 edge. The position of the hydride was calculated to be 1.11 Å below the plane of the metal atoms and *trans* to CO13 and CO33. This is a general feature of metal clusters;[1,4,10–13] when a metal–metal edge contains a bridging hydride and a single atom bridge from an organic ligand, that edge will

(6) Day, M.; Kabir, S. E.; Wolf, E.; Rosenberg, E. *J. Cluster Sci.* **1990**, *1*, 355.
(7) (a) Ditzel, S. J.; Johnson, B. F. G.; Lewis, J. *J. Chem. Soc., Dalton Trans.* **1987**, 1293. (b) Kaesz, H. D.; Knobler, C. B.; Andrews, M. A.; van Buskirk, G.; Szostak, R.; Strouse, C. E.; Lin, Y. C.; Mayr, A. *Pure Appl. Chem.* **1982**, *54*, 131.
(8) Bryan, E. G.; Johnson, B. F. G.; Lewis, J. *J. Chem. Soc., Dalton Trans.* **1977**, 1328.
(9) Yin, C. C.; Deeming, A. J. *J. Chem. Soc., Dalton Trans.* **1975**, 2091.
(10) Azam, K. A.; Yin, C. C.; Deeming, A. J. *J. Chem. Soc., Dalton Trans.* **1978**, 1201.
(11) Day, M. W.; Hajela, S.; Hardcastle, K. I.; McPhillips, T.; Botta, M.; Gobetto, R.; Milone, L.; Osella, D.; Gellert, R. W. *Organometallics* **1990**, *9*, 913.
(12) Adams, R. D.; Tanner, J. T. *Organometallics* **1988**, *7*, 2241.

be shortened and the hydride will be well below the plane of the metals. This feature of the bonding in metal clusters allows the metal atoms to maintain approximate octahedral geometry. The organic ligand serves as a three electron donor through two equivalent bonds from N to Os1 and Os2 (N–Os1 = N–Os3 = 2.15(1) Å).

The reaction of di-*n*-propylamine with **1** at 40–45 °C in benzene for 8 h yields the μ-imidoyl complex $(\mu\text{-H})(\mu\text{-}\eta^2\text{-}CH_3CH_2C{=}NCH_2CH_2CH_3)Os_3(CO)_{10}$ (**11**) in 44% yield. Interestingly, we do not observe formation of an N–H oxidative addition product analogous to **9** in this case. As with **10** we do obtain $(\mu\text{-H})_2Os_3(CO)_{10}$[3] (2%) and in addition we obtain $(\mu\text{-H})(\mu\text{-OH})Os_3(CO)_{10}$[14] (6%) and trace amounts of $Os_3(CO)_{12}$. With other acyclic aliphatic secondary amines containing shorter alkyl groups, we observe products which are the result of α- and β-carbon–hydrogen bond activation.[1,15] This suggests that the presence of a γ-carbon atom sterically interferes with β-carbon–hydrogen bond activation. In the case of pyrrolidine reacting with **1**, it seems reasonable that an α-carbon–hydrogen bond activation is observed since the β-carbons are "tied back", making the β-hydrogens inaccessible to the metal atoms after coordination of the amine. At room temperature, in methylene chloride, for 24 h, the reaction of di-*n*-propylamine with **1** yields **11** in somewhat lower yield (35%) with a commensurate increase in the coproducts $(\mu\text{-H})_2Os_3(CO)_{10}$ (4%) and $(\mu\text{-H})(\mu\text{-OH})Os_3(CO)_{10}$ (10%). Compound **11** can also be prepared in comparable yields (42%) by the reaction of $(\mu\text{-H})(\mu\text{-}\eta^2\text{-}CHCH_2)Os_3(CO)_{10}$[16] with di-*n*-propylamine in refluxing benzene for 8 h. This probably proceeds by reductive elimination of ethylene followed by rapid reaction of the amine with the coordinately unsaturated $Os_3(CO)_{10}$ intermediate. Although this route to **11** is uncomplicated by coproducts, the synthesis of $(\mu\text{-H})(\mu\text{-}\eta^2\text{-}CHCH_2)Os_3(CO)_{10}$ from $(\mu\text{-H})_2Os_3(CO)_{10}$ and acetylene is not a high yield reaction,[16] making direct reaction of the amine with **1** the preferred route. Decarbonylation of **11** to give **3** proceeds thermally or photochemically as for **10** to give **3** in 92–93% yield.

B. Reactivity of 2 and 3 with Alkyl Isocyanides. Compound **2** reacts with methyl isocyanide at room temperature to give a single product in 96% yield. The ^{1}H-NMR, infrared, and elemental analyses are consistent with the formula $(\mu\text{-H})(\mu\text{-}\eta^2\text{-}\overline{C{=}NCH_2CH_2CH_2}\,)Os_3(CO)_9(CNCH_3)$ (**12**). The exact disposition of the isocyanide ligand could not be ascertained from these data and so a solid-structure determination of **12** was undertaken. The structure of **12** is shown in Figure 3, crystal data are given in Table I, atomic coordinates are in Table VI, and selected distances and bond angles in Table VII. The solid-state structure reveals that the isocyanide ligand has added to the cluster on the osmium atom formerly bound to the C=N bond of the imidoyl ligand. It occupies an axial position directly *trans* to CO22 and on the same face of the cluster as the μ-imidoyl ligand. The preference of isocyanide ligands for axial coordination sites on trimetallic clusters is well-known.[17–19] It is more difficult to understand why the isocyanide coordinates to the same face of the metal cluster as the μ-imidoyl ligand, unless **12** is the kinetic product, which it is not (vide infra). As previously

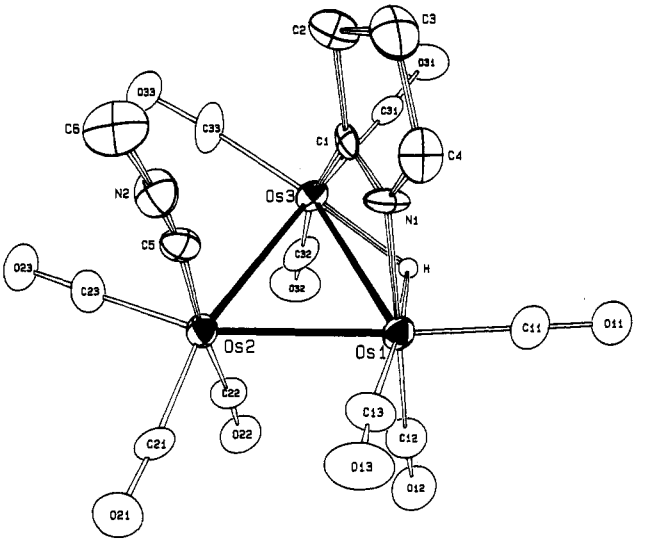

Figure 3. ORTEP drawing of $(\mu\text{-H})(\mu\text{-}\eta^2\text{-}\overline{C{=}NCH_2CH_2CH_2}\,)Os_3(CO)_9(CNCH_3)$ (**12**) showing the calculated position of the hydride.

Table VI. Fractional Atomic Coordinates for $(\mu\text{-H})(\mu\text{-}\eta^2\text{-}\overline{C{=}NCH_2CH_2CH_2}\,)Os_3(CO)_9(CNCH_3)$ (12)

atom	*x*	*y*	*z*	*B* (Å^2)[a]
Os1	0.17589(9)	0.31627(5)	0.08947(6)	3.58(2)
Os2	0.24527(8)	0.2522695)	0.27164(5)	3.61(2)
Os3	0.01322(9)	0.17324(5)	0.15889(6)	3.46(2)
O11	0.086(2)	0.372(1)	–0.107(1)	7.4(5)
O12	0.464(2)	0.248(1)	0.019(1)	7.9(5)
O13	0.315(2)	0.477(1)	0.163(1)	8.5(5)
O21	0.497(2)	0.366(1)	0.349(1)	7.5(5)
O22	0.467(2)	0.135(1)	0.188(1)	6.7(4)
O23	0.226(2)	0.148(1)	0.448(1)	6.5(4)
O31	–0.246(2)	0.105(1)	0.035(1)	6.9(4)
O32	0.215(2)	0.020(1)	0.121(1)	7.9(5)
O33	–0.097(2)	0.111(1)	0.340(1)	6.0(4)
N1	–0.034(1)	0.346(1)	0.134(1)	4.3(4)
N2	0.011(2)	0.380(1)	0.354(1)	5.2(5)
C1	–0.104(2)	0.287(1)	0.164(1)	3.1(4)
C2	–0.263(2)	0.307(1)	0.199(2)	5.0(5)
C3	–0.276(2)	0.400(2)	0.170(2)	6.6(6)
C4	–0.120(3)	0.427(1)	0.137(2)	5.3(6)
C5	0.091(2)	0.334(1)	0.319(1)	4.3(5)
C6	–0.076(2)	0.433(1)	0.402(2)	6.4(6)
C11	0.122(3)	0.349(1)	–0.033(2)	5.3(6)
C12	0.365(2)	0.274(1)	0.047(1)	5.3(5)
C13	0.264(2)	0.415(1)	0.139(2)	5.4(6)
C21	0.402(2)	0.328(1)	0.317(1)	4.7(5)
C22	0.375(2)	0.178(1)	0.218(1)	4.4(5)
C23	0.235(3)	0.187(2)	0.381(2)	5.5(6)
C31	–0.152(2)	0.133(2)	0.079(1)	5.2(5)
C32	0.141(2)	0.078(1)	0.135(2)	5.3(5)
C33	–0.061(3)	0.133(1)	0.271(1)	5.3(6)
H	0.097	0.214	0.054	4.0*

[a] The starred value refers to the atom that was refined isotropically. Anisotropically refined atoms are given in the form of the isotropic equivalent displacement parameter defined as $(4/3)[a^2B(1,1) + b^2B(2,2) + c^2B(3,3) + ab(\cos\gamma)B(1,2) + ac(\cos\beta)B(1,3) + bc(\cos\alpha)B(2,3)]$.

(13) (a) Day, M. W.; Hardcastle, K. I.; Deeming, A. J.; Arce, A. J.; DeSanctis, Y.; *Organometallics* **1990**, *9*, 6. (b) Deeming, A. J.; Arce, A. J.; DeSanctis, Y.; Day, M. W.; Hardcastle, K. I. *Organometallics* **1989**, *8*, 1408.

(14) (a) Johnson, B. F. G.; Lewis, J.; Kilty, O. A. *J. Chem. Soc. A* **1968**, 2859. (b) Arce, A. J.; Deeming, A. J.; Donovan-Mtunzi, S.; Kabir, S. E. *J. Chem. Soc., Dalton Trans.* **1985**, 2479. (c) Dossi, C.; Fusi, A.; Pizzotti, M.; Psaro, R. *Organometallics* **1990**, *9*, 1994.

(15) Kabir, S. E.; Day, M.; Irving, M.; McPhillips, T.; Minassian, H.; Rosenberg, E.; Hardcastle, K. I. *Organometallics* **1991**, *10*, 3997.

(16) Deeming, A. J.; Hasso, S.; Underhill, M. *J. Chem. Soc., Dalton Trans.* **1975**, 1614.

(17) (a) Adams, R. D.; Golembeski, N. M. *J. Am. Chem. Soc.* **1979**, *101*, 2579. (b) Adams, R. D.; Golembeski, N. M. *Inorg. Chem.* **1979**, *18*, 1909.

(18) Bruce, M. I.; Matisons, J. G.; Wallis, R. C.; Patrick, J. M.; Skelton, B. W.; White, A. H. *J. Chem. Soc., Dalton Trans.* **1983**, 2365.

(19) Ma, A. K.; Einstein, F. W. B.; Johnston, V. J.; Pomeroy, R. K. *Organometallics* **1990**, *9*, 45.

Table VII. Selected Bond Distances (Å) and Angles (deg) for (μ-H)(μ-η^2-C=NCH$_2$CH$_2$CH$_2$)Os$_3$(CO)$_9$(CNCH$_3$) (12)[a]

Distances			
Os1–Os2	2.861(1)	N1–C1	1.23(2)
Os1–Os3	2.929(1)	C1–C2	1.57(3)
Os2–Os3	2.872(1)	C2–C3	1.54(3)
Os1–N1	2.08(1)	C3–C4	1.56(3)
Os2–C5	2.05(2)	C4–N1	1.52(3)
Os3–C1	2.12(2)	C5–N2	1.16(3)
Os1–H	1.85	N2–C6	1.38(3)
Os3–H	1.85	Os–C(CO)	1.92(4)[b]
		C–O(CO)	1.14(3)[b]
Angles			
Os1–Os2–Os3	61.45(3)	C2–C3–C4	107(2)
Os1–Os3–Os2	59.10(3)	N1–C4–C3	104(2)
Os2–Os1–Os3	59.45(3)	C1–N1–C4	112(2)
N1–C1–C2	116(2)	C5–N2–C6	175(2)
C1–C2–C3	100(2)	Os–C–O(CO)	176(2)[b]

[a] Numbers in parentheses are estimated standard deviations in the least significant digits. [b] Average values.

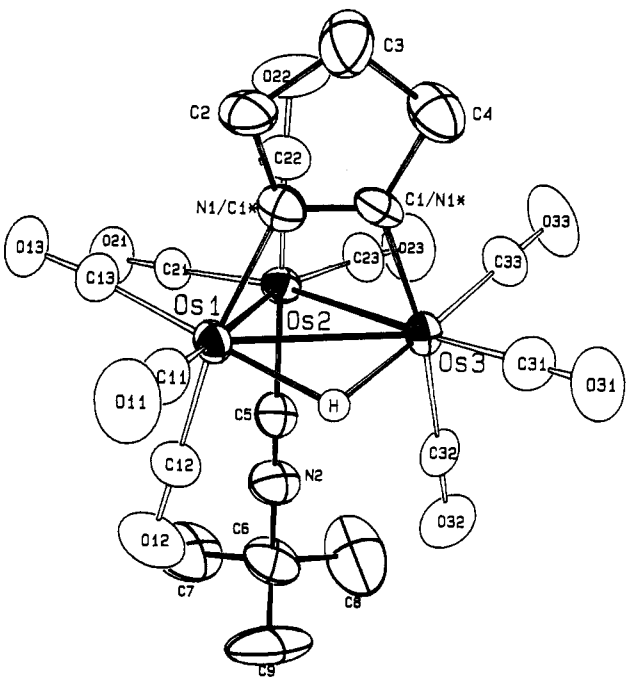

Figure 4. ORTEP drawing of (μ-H(μ-η^2-C=NCH$_2$CH$_2$CH$_2$)Os$_3$CO$_9$CNCCH$_3$)$_3$) (**13**) showing the calculated position of the hydride. Atoms marked with an asterisk represent equal populations of disordered carbon and nitrogen atoms bound to the metal.

observed,[17,19] the osmium–isocyanide carbon bond (Os2–C5 = 2.05(2) Å) is significantly longer than the average osmium–carbonyl carbon bond (1.92(2) Å). In other respects **12** is virtually identical to the previously reported **10**, having very similar metal–metal, metal–ligand, and intraligand bond distances.[1]

In order to ascertain whether the steric bulk of the alkyl group on the isocyanide played a role in determining the structure of isocyanide adducts of **2**, as we observed with the phosphine adducts of **2**,[2] we reacted *tert*-butyl isocyanide with **2**. The reaction of **2** with *tert*-butyl isocyanide proceeds at room temperature to give a single major product in 92% yield whose ^{1}H-NMR, infrared, and elemental analysis are consistent with the formula (μ-H)(μ-η^2-C=NCH$_2$CH$_2$CH$_2$)Os$_3$(CO)$_9$(CNC(CH$_3$)$_3$) (**13**). The solid-state structure of **13** is shown in Figure 4, crystal data are given in Table I, atomic coordinates are in Table VIII, and selected distances and bond angles are in Table IX. As can be seen from Figure 4, the overall structure of **13** is very similar to that of **12**; however, there is disordering with respect to the location of C1 and N1 in this structure. To our knowledge this is the first time methyl and *tert*-butyl isocyanide complexes have been structurally compared in directly analogous triosmium systems. The effect of replacing the methyl group with

Table VIII. Fractional Atomic Coordinates for (μ-H)(μ-η^2-C=NCH$_2$CH$_2$CH$_2$)Os$_3$(CO)$_9$(CNC(CH$_3$)$_3$) (13)[a]

atom	x	y	z	B (Å^2)
Os1	0.14563(4)	0.23292(2)	0.39884(2)	2.563(7)
Os2	–0.05672(4)	0.23593(2)	0.49773(2)	2.469(7)
Os3	–0.15687(4)	0.31029(2)	0.31641(2)	2.484(7)
O11	0.368(1)	0.2374(6)	0.2981(6)	6.6(3)
O12	0.045(1)	0.0860(5)	0.3278(7)	6.3(3)
O13	0.403(1)	0.1834(5)	0.5969(6)	5.2(2)
O21	0.125(1)	0.1437(5)	0.6745(5)	5.1(2)
O22	0.118(1)	0.3652(5)	0.6097(5)	6.2(2)
O23	–0.3454(9)	0.2718(5)	0.5339(5)	5.8(2)
O31	–0.257(1)	0.3940(4)	0.1285(5)	5.4(2)
O32	–0.4041(9)	0.1971(5)	0.2141(5)	4.5(2)
O33	–0.368(1)	0.3932(5)	0.3836(6)	6.0(2)
N2	–0.248(1)	0.1029(5)	0.3914(6)	4.5(2)
N1/C1*	0.182(1)	0.3398(5)	0.4250(6)	3.0(2)
C1/N1*	0.046(1)	0.3732(4)	0.3871(5)	2.9(2)
C2	0.325(1)	0.3861(6)	0.4706(8)	4.2(3)
C3	0.257(2)	0.4577(8)	0.460(1)	6.1(4)
C4	0.071(1)	0.4504(6)	0.3976(8)	4.6(3)
C5	–0.174(1)	0.1513(5)	0.4259(6)	3.3(2)
C6	–0.348(2)	0.0396(6)	0.356(1)	5.5(4)
C7	–0.262(3)	–0.0143(8)	0.437(1)	9.6(7)
C8	–0.529(2)	0.059(1)	0.340(2)	11.4(8)
C9	–0.337(2)	0.0176(9)	0.263(1)	9.2(6)
C11	0.284(1)	0.2384(6)	0.3334(7)	3.7(2)
C12	0.080(1)	0.1426(6)	0.3565(7)	3.8(2)
C13	0.305(1)	0.2046(6)	0.5250(7)	3.4(2)
C21	0.055(1)	0.1766(5)	0.6080(6)	2.8(2)
C22	0.059(1)	0.3161(6)	0.5656(7)	3.7(2)
C23	–0.237(1)	0.2604(6)	0.5238(7)	3.9(3)
C31	–0.216(1)	0.3635(6)	0.1988(7)	3.6(2)
C32	–0.313(1)	0.2397(5)	0.2528(6)	2.9(2)
C33	–0.288(1)	0.3616(6)	0.3599(7)	3.5(2)
H	–0.022	0.260	0.280	6.0*

[a] The starred value refers to the atom that was refined isotropically. Anisotropically refined atoms are given in the form of the isotropic equivalent displacement parameter defined as $(4/3)[a^2B(1,1) + b^2B(2,2) + c^2B(3,3) + ab(\cos\gamma)B(1,2) + ac(\cos\beta)B(1,2) + bc(\cos\alpha)B(2,3)]$.

Table IX. Selected Bond Distances (Å) and Angles (deg) for (μ-H)(μ-η^2-C=NCH$_2$CH$_2$CH$_2$)Os$_3$(CO)$_9$(CNC(CH$_3$)$_3$) (13)[a]

Distances			
Os1–Os2	2.8672(6)	N1/C1*–C2	1.48(1)
Os1–Os3	2.9127(5)	C2–C3	1.50(2)
Os2–Os3	2.8708(5)	C3–C4	1.55(2)
Os1–N1/C1*	2.11(1)	C4–C1/N1*	1.51(1)
Os3–C1–N1*	2.086(8)	N1/C1*–C1/N1*	1.30(1)
Os2–C5	2.000(9)	C5–N2	1.14(1)
Os1–H	1.85	N2–C6	1.48(2)
Os3–H	1.85	C6–C7	1.54(2)
Os–C(CO)	1.91(2)[b]	C6–C8	1.62(3)
C–O(CO)	1.13(2)[b]	C6–C9	1.53(3)
Angles			
Os1–Os2–Os3	61.01(1)	C5–N2–C6	174(1)
Os1–Os3–Os2	59.43(1)	N2–C6–C7	105(1)
Os2–Os1–Os3	59.56(1)	N2–C6–C8	107(1)
C1/N1*–N1/C1*–C2	112.7(9)	N2–C6–C9	106(1)
N1/C1*–C2–C3	105.6(9)	C7–C6–C8	114(2)
C2–C3–C4	106(1)	C7–C6–C9	110(1)
C3–C4–C1/N1*	103.1(9)	C8–C6–C9	114(1)
N1/C1*–C1/N1*–C4	112.1(8)	Os–C–O(CO)	176(2)[b]

[a] Numbers in parentheses are estimated standard deviations in the least significant digits. [b] Average values.

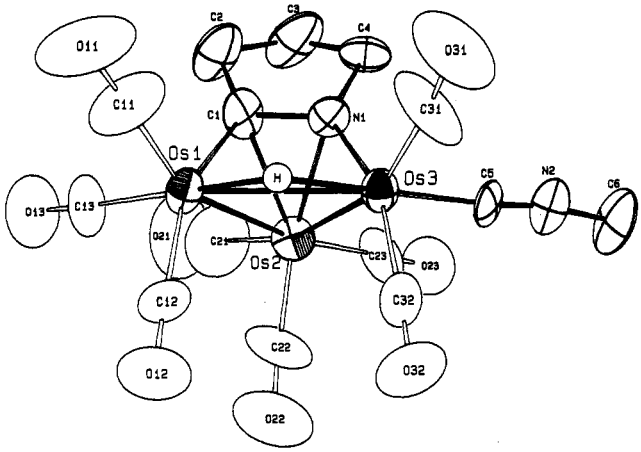

Figure 5. ORTEP drawing of (μ-H)(μ_3-η^2-C=NCH$_2$CH$_2$CH$_2$)Os$_3$(CO)$_8$(CNCH$_3$) (**16**) showing the calculated position of the hydride.

Scheme II

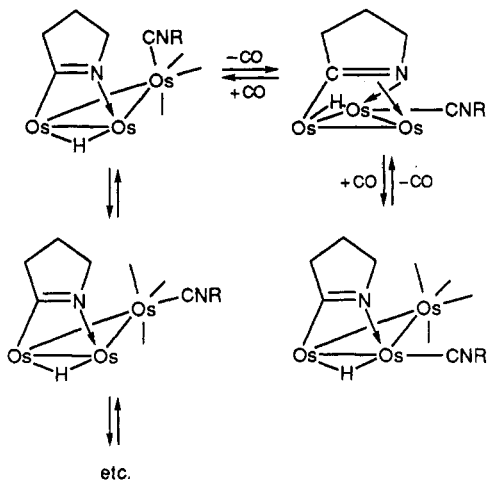

the bulkier *tert*-butyl group is to make the isocyanide ligand occupy the axial site on the face of the triangle opposite that of the imidoyl ligand. We feel this difference is best understood in terms of intramolecular crowding rather than crystal packing effects.

The ^{1}H-NMR of **12** shows one major isomer (relative intensity = 0.81) in solution with a hydride signal at −14.68 ppm. In addition, we observe six additional hydride resonances at −14.69, −14.74, −14.96, −14.98, −15.64, and −16.52 ppm (relative intensity = 0.05, 0.05, 0.03, 0.04, 0.01, 0.02). None of these resonances correspond to **2** or **10**. If one allows for slow carbonyl dissociation–association in solution and a restricted windshield wiper motion pivoted on the carbon of the imidoyl ligand, there can be seven positional isomers, as observed (Scheme II). The ^{1}H-NMR spectrum of **12** remains essentially unchanged at −50 °C except for a slight decrease in the populations of the minor isomers. Interestingly, **13** shows one major isomer in solution with a hydride resonance at −14.89 ppm (relative intensity = 0.88) but only three minor isomers are observed with hydride resonances at −14.77, −14.98, and −15.01 ppm (relative intensity = 0.02, 0.04, 0.06). The observation of only four positional isomers for **13** could be due to either much slower CO dissociation in **13** relative to **12** or more likely a very low population in **13** of the isomers where the isocyanide is on the osmium atom bound to the nitrogen of the imidoyl ligand (Scheme II). The reaction of **3** with methyl or *tert*-butyl isocyanide at room temperature

Table X. Fractional Atomic Coordinates for (μ-H)(μ_3-η^2-C=NCH$_2$CH$_2$CH$_2$)Os$_3$(CO)$_8$(CNCH$_3$) (16)

atom	x	y	z	B (Å^2)[a]
Os1	−0.27387(7)	0.32027(4)	0.11903(6)	3.35(1)
Os2	−0.07921(8)	0.21835(4)	−0.16200(6)	3.77(1)
Os3	0.07868(7)	0.20888(4)	0.06768(6)	3.07(1)
O11	−0.362(2)	0.474(1)	0.338(2)	12.0(5)
O12	−0.457(2)	0.1898(8)	0.390(1)	7.1(4)
O13	−0.568(2)	0.400(1)	−0.015(2)	8.3(5)
O21	−0.284(2)	0.297(1)	−0.398(2)	11.9(7)
O22	−0.265(2)	0.0749(9)	0.028(2)	10.4(5)
O23	0.213(2)	0.1005(9)	−0.426(1)	7.7(4)
O31	0.240(2)	0.278(1)	0.265(2)	9.0(4)
O32	−0.024(2)	0.0555(8)	0.321(1)	7.9(4)
N1	0.072(1)	0.3037(7)	−0.135(1)	3.3(3)
N2	0.428(2)	0.0897(9)	−0.166(1)	5.1(4)
C1	−0.092(2)	0.358(1)	−0.103(1)	4.0(3)
C2	−0.083(2)	0.435(1)	−0.238(2)	6.1(5)
C3	0.098(3)	0.404(1)	−0.381(2)	7.4(6)
C4	0.209(2)	0.3401(9)	−0.281(2)	4.2(4)
C5	0.297(2)	0.1316(9)	−0.086(2)	4.0(4)
C6	0.574(2)	0.031(1)	−0.277(2)	6.6(6)
C11	−0.325(3)	0.415(1)	0.259(2)	7.1(6)
C12	−0.392(2)	0.2400(9)	0.285(2)	4.1(4)
C13	−0.460(2)	0.369(1)	0.037(2)	5.9(5)
C21	−0.217(3)	0.265(2)	−0.305(2)	8.6(7)
C22	−0.196(2)	0.131(1)	−0.052(2)	6.4(4)
C23	0.107(2)	0.144(1)	−0.328(2)	5.4(5)
C31	0.186(2)	0.248(1)	0.18692)	6.6(5)
C32	0.017(2)	0.112(1)	0.226(2)	4.5(4)
H	−0.115	0.276	0.227	4.0*

[a] The starred value refers to the atom that was refined isotropically. Anisotropically refined atoms are given in the form of the isotropic equivalent displacement parameter defined as isotropic equivalent displacement parameter defined as $(4/3)[a^2B(1,1) + b^2B(2,2) + c^2B(3,3) + ab(\cos\gamma)B(1,2) + ac(\cos\beta)B(1,3) + bc(\cos\alpha)B(2,3)]$.

proceeds as for **2**, yielding the addition products (μ-H)(μ-η^2-CH$_3$CH$_2$C=NCH$_2$CH$_2$CH$_3$)Os$_3$(CO)$_9$(CNR) (R = CH$_3$, **14**; R = C(CH$_3$)$_3$, **15**) in 96 and 90% yields, respectively. Compounds **14** and **15** appear to be structurally identical with **12** and **13** on the basis of their infrared and ^{1}H-NMR spectra. As for **12**, **14** shows one major isomer in solution with a hydride resonance at −14.28 (relative intensity = 0.72) and six minor isomers at −14.29, −14.37, −14.55, −14.56, −14.76, and −16.33 ppm (relative intensity = 0.05, 0.04, 0.03, 0.04, 0.04, and 0.08). Similarly, as for **13**, **15** shows one major isomer in solution, with a hydride resonance at −14.49 ppm (relative intensity = 0.76) and three minor isomers at −14.56, −14.58, and −16.16 ppm (relative intensity = 0.03, 0.05, 0.14). It is apparent from these results that the geometries of the isocyanide adducts **12**–**15** do not show as much sensitivity to the structure of the imidoyl ligand as observed for the bulkier phosphine ligand in **4**–**6**.[2]

Thermolysis of **12**–**15** at 128 °C for 8–12 h leads to decarbonylation and formation of the corresponding μ_3-imidoyl complexes (μ-H)(μ_3-η^2-C=NCH$_2$CH$_2$CH$_2$)Os$_3$(CO)$_8$(CNR) (R = CH$_3$, **16** (51%); R = C(CH$_3$)$_3$, **17** (51%)) and (μ-H)(μ_3-η^2-CH$_3$CH$_2$C=NCH$_2$CH$_2$CH$_3$)Os$_3$(CO)$_8$(CNR) (R = CH$_3$, **18** (77%); R = C(CH$_3$)$_3$, **19** (80%)). In contrast to the thermolysis of **4** and **5** we observe the formation of small amounts of **2**, **3**, **10**, and **11** in the thermolysis of **12**–**15**, showing that isocyanide dissociation is somewhat competitive with carbonyl dissociation.

An X-ray crystallographic investigation of **16** was undertaken to ascertain the exact location of the isocyanide ligand on the cluster. The solid-state structure of **16** is shown in Figure 5, crystal data are given in Table I, atomic coordinates are in Table X, and selected distances and

Table XI. Selected Bond Distances (Å) and Angles (deg) for $(\mu\text{-H})(\mu_3\text{-}\eta^2\text{-}\overline{C{=}NCH_2CH_2CH_2}\overline{)}Os_3(CO)_8(CNCH_3)$ (16)[a]

		Distances	
Os1–Os2	2.7643(7)	N1–C1	1.38(2)
Os1–Os3	2.9501(8)	C1–C2	1.51(2)
Os2–Os3	2.7288(9)	C2–C3	1.56(2)
Os1–C1	2.04(1)	C3–C4	1.56(2)
Os2–C1	2.29(2)	C4–N1	1.50(2)
Os2–N1	2.19(1)	C5–N2	1.14(2)
Os3–N1	2.09(1)	N2–C6	1.42(2)
Os3–C5	2.01(1)	Os–C(CO)	1.89(3)[b]
Os1–H	1.85	C–O(CO)	1.14(2)[b]
Os3–H	1.85		
		Angles	
Os1–Os2–Os3	64.96(2)	C4–N1–C1	113(1)
Os1–Os3–Os2	58.10(2)	N1–C1–C2	109(1)
Os2–Os1–Os3	56.94(2)	C1–C2–C3	103(1)
C5–N2–C6	169(2)	C2–C3–C4	104(1)
Os–C–O(CO)	176(2)[b]	C3–C4–N1	101(1)

[a] Numbers in parentheses are estimated standard deivations in the least significant digits. [b] Average values.

bond angles are in Table XI. The structure of **16** consists of a triangle of osmium atoms with one elongated edge (Os1–Os3 = 2.950(1) Å) and two shorter edges Os1–Os2 = 2.764(1) Å and Os2–Os3 = 2.723(1) Å). The hydride ligand was located along the Os1–Os3 edge using the program Hydex[5] and is almost in plane with the osmium triangle. The isocyanide ligand is located on Os3 almost directly *trans* to the hydride. This is in contrast to the related complex **8** where the more bulky phosphine is *cis* to the hydride.[2] This *cis* orientation of more bulky ligands appears to be quite general and is thought to be the consequence of minimization of steric crowding of the phosphine with metal–metal bond vectors.[20] In the absence of such crowding (i.e. with the less bulky isocyanides) it appears that better σ donors than carbonyl prefer to be *trans* to the hydride ligand. The imidoyl metal–carbon and metal–nitrogen distances are significantly shorter in **16** *versus* **8** (2.04(1) and 2.09(1) Å in **16** and 2.08(1) and 2.13(1) Å in **8**) which probably also reflects the greater steric crowding between the imidoyl ligand and the bulkier phosphine ligand. Interestingly, the Os2–C1 and Os2–N1 bond lengths in **16** are virtually identical to those in **8**, as is the C1–N1 bond length, suggesting that the longer Os1–C1 and Os3–N1 bond lengths in **8** are not compensated for by a stronger bonding interaction with Os2.[2]

1D and 2D Nuclear Magnetic Resonance Studies of 10, 2, and 16–19. In recent years it has been shown that two-dimensional magnetization transfer experiments can be very useful for elucidating multistage ligand exchange processes in polynuclear transition metal clusters.[21] In light of the complex multistage ligand exchange processes observed for the ruthenium analogs of **2** and the complex variable temperature one-dimensional spectra obtained for **16–19** (vide infra) we undertook ^{13}C-EXSY investigations of **10** and **2** and ^{1}H-EXSY investigations of **17–19**.

Compound **10** is rigid on the NMR time scale at room temperature. The $^{13}C\{^1H\}$-NMR of a 30% ^{13}CO-enriched sample shows the expected ten resonances at 186.01, 183.50, 179.18, 177.54, 175.01, 174.80, 174.71, 174.26, 174.20, and 173.87 ppm. From the proton-coupled spectrum we can assign the resonances at 174.20 and 173.87 ppm to the carbonyls *trans* to the bridging hydride ($^2J(^1H-^{13}C)$ = 10.7 and 12.3 Hz, respectively) and the two resonances at 175.01 and 174.71 ppm to the equatorial carbonyls *cis* to the bridging hydride ($^2J(^1H-^{13}C)$ = 2.7 and 2.9 Hz, respectively). The two resonances at 179.19 and 177.54 ppm, which show barely resolvable coupling with the hydride ($^2J(^1H-^{13}C)$ = ~1 Hz), are assigned to the axial carbonyls at the hydride-bridged edge on the basis of the fact that axial carbonyls are generally found at a lower field than equatorial carbonyls on a given metal center in trinuclear clusters.[22] The two resonances at 186.01 and 183.50 ppm, which show large $^{13}C-^{13}C$ coupling satellites ($^2J(^{13}C-^{13}C)$ = 35.2 and 35.1 Hz, respectively), are assigned to the two mutually *trans* axial carbonyl groups of the $Os(CO)_4$ group, and by process of elimination the resonances at 174.8 and 174.35 ppm are assigned to the equatorial carbonyl groups of this osmium atom. We cannot differentiate the carbonyl groups on the osmium atom bound to the carbon of the μ-imidoyl ligand from those on the osmium atom bound to nitrogen.

With these assignments in hand we then examined the ^{13}C-EXSY spectra of **10** (Figure 6). At 295 K no off-diagonal peaks are observed except for two relatively low intensity scalar coupling crosspeaks between the satellites around the resonances assigned to the mutually *trans* carbonyls on the $Os(CO)_4$ unit. At 303 K off-diagonal peaks are observed between one of these axial carbonyl groups (at 183.50 ppm) and the two equatorial carbonyl groups on $Os(CO)_4$ (at 174.80 and 174.26 ppm) (Figure 6a), indicating the onset of a tripodal exchange process between these carbonyl groups. At 313 K two additional lower intensity off-diagonal peaks are observed (Figure 6b) between the equatorial carbonyls and the other axial carbonyl group on the $Os(CO)_4$ group (at 186.01 ppm). This type of sequential tripodal exchange has been previously observed in $Os(CO)_4$ groups in triosmium clusters.[23] No other evidence of exchange is observed up to 333 K. These results give evidence for the rigid nature of the imidoyl and hydride ligands in **10** and related clusters.[1,2,4]

The low temperature limiting ^{13}C-NMR spectrum of a 30% ^{13}CO-enriched sample of **2** is approached at 188 K (Figure 7), revealing the expected nine resonances of approximately equal intensity at 179.68, 178.88, 177.42, 174.11, 173.68, 173.21, 171.90, 171.05, and 168.88 ppm. Using the same arguments as outlined above for **10**, we can assign the resonances at 171.90 and 171.03 ppm to the carbonyl groups *trans* to the hydride ($^2J(^1H-^{13}C)$ = 10.2 and 12.2 Hz, respectively), the resonances at 174.11 and 168.88 ppm ($^2J(^1H-^{13}C)$ = 4.3 and 4.1 Hz, respectively) to the equatorial carbonyl groups *cis* to the bridging hydride, the resonances at 178.88 and 177.42 ppm ($^2J(^1H-^{13}C)$ = 2.6 and 3.2 Hz) to the axial carbonyls on the hydride-bridged edge of the clusters, the resonances at 173.68 and 173.26 ppm to the radial carbonyl groups on the osmium atom not bridged by the hydride and π-bound to the imidoyl ligand, and the resonances at 179.68 ppm to the axial carbonyl at this same osmium atom. As the temperature is increased to 233 K, the resonances at 179.68, 173.68 and 173.21 ppm broaden into the baseline and

(20) Deeming, A. J.; Donovan-Mtunzi, S.; Kabir, S. E.; Hursthouse, M. B.; Malik, K. M. A.; Walker, N. P. C. *J. Chem. Soc., Dalton Trans.* **1987**, 1869.

(21) Farrugia, L. J.; Rae, S. E. *Organometallics* **1992**, *11*, 196 and references therein.

(22) Mann, B. E.; Taylor, B. F. *^{13}C NMR Data for Organic Compounds*; Academic: New York, 1981; p 176.

(23) Pomeroy, R. K.; Alex, R. F. *Organometallics* **1987**, *6*, 2437.

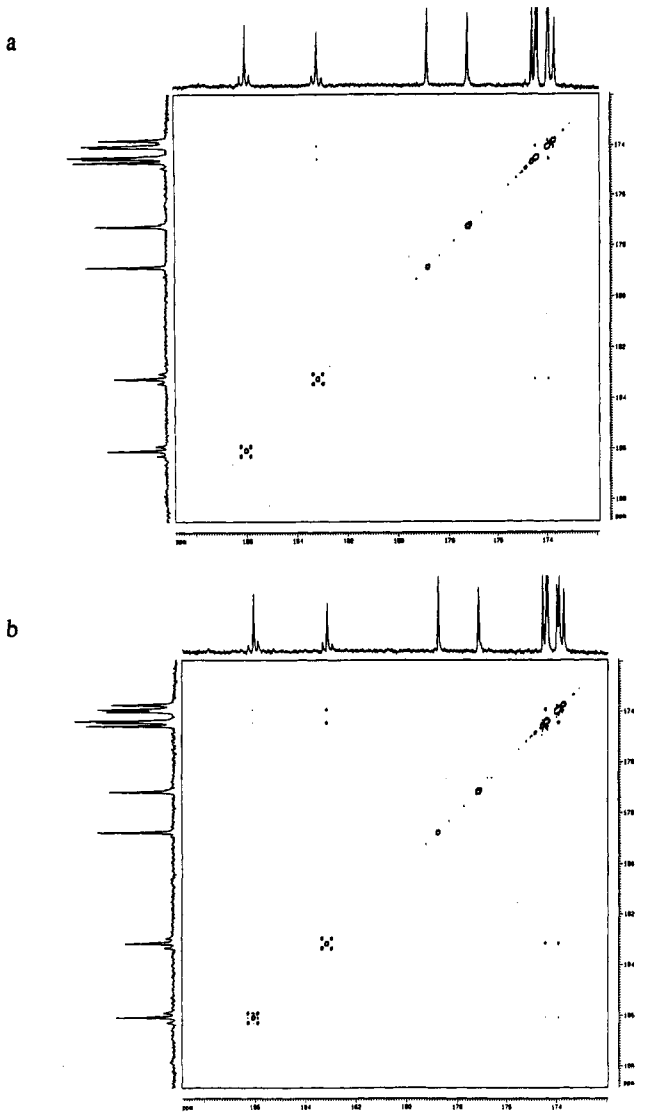

Figure 6. ^{13}C-ESXY spectra of **10** at 90 MHz in $CDCl_3$: (a) 303 K (mixing time = 1.0 s; (b) 313 K (mixing time = 1.0 s).

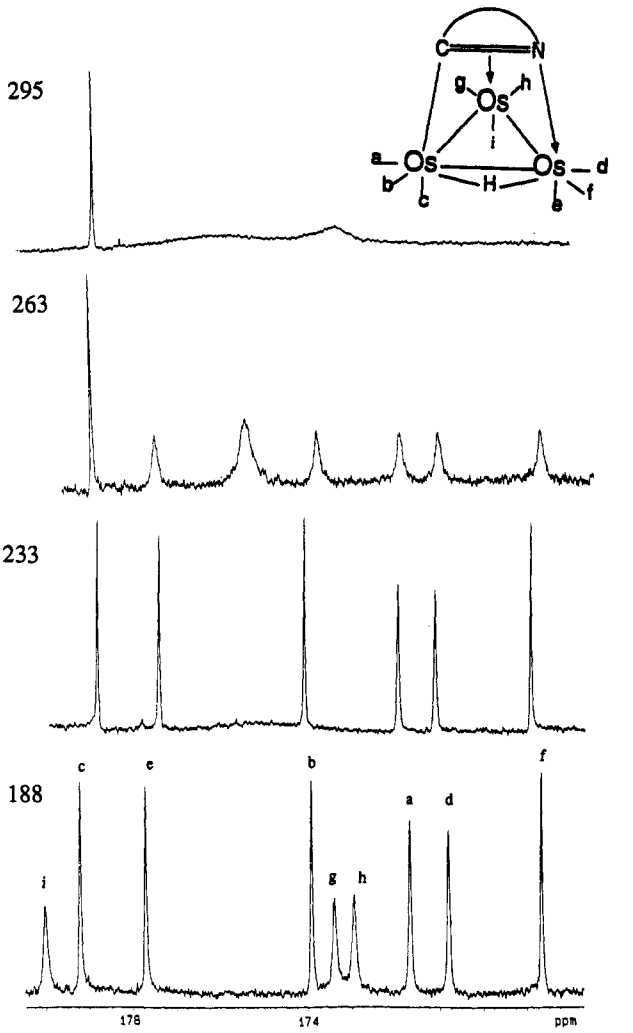

Figure 7. Variable temperature ^{13}C-NMR of **2** at 90 MHz in CD_2Cl_2.

eventually reemerge as a broad resonance at 175.52 ppm at 263 K. In the temperature range 188–233 K the remaining six resonances are relatively sharp, while in the temperature range 233–263 K all the resonances except the one at 178.90 ppm begin to broaden. At 295 K all of the resonances have broadened into the baseline except the one at 178.90 ppm, which remains sharp. The general pattern of fluxionality observed for **2** is consistent with the lowest energy exchange process being axial–radial tripodal exchange at the unique osmium atom followed by the onset of a windshield wiper motion pivoting on the carbon atom of the imidoyl ligand accompanied by hydride edge hopping and overlapping with onset of axial–radial tripodal exchange at the osmium atom bound to the nitrogen. That the resonance at 178.88 ppm remains sharp throughout the temperature range examined suggests that this resonance can be assigned to the axial carbonyl on the osmium atom σ-bound to the carbon of the imidoyl ligand and that there is no tripodal motion of the carbonyls at this osmium atom. This overall fluxional behavior is directly analogues to that previously reported for $(\mu$-H)-$Ru_3(CO)_9(CH_3C{=}NCH_2CH_3)$.[24]

In order to gain further information on the relative energies of the different stages of the exchange processes in **2** and to more definitively assign the carbonyl resonances, we have obtained ^{13}C-EXSY spectra of **2** at 188, 233, and 263 K. At 188 K with a mixing time of 0.5 s we observe off-diagonal elements for only the three carbonyl groups at 179.68, 173.68, and 173.21 ppm assigned to the carbonyls on the π-bound osmium atom of **2** (Figure 8a). At 233 K, at which temperature the three resonances due to the carbonyl groups on the π-bound osmium atom are broadened into the baseline, we observe intense off-diagonal elements between the resonances at 174.11 and 171.90 ppm (Figure 8b). These must be due to the onset of the windshield wiper motion which would be expected to average the two radial carbonyls on the osmium atom σ-bound to the carbon of the imidoyl ligand. Taking the carbon–hydrogen coupling information discussed above into account, we can definitively assign the resonance at 171.90 ppm to the radial carbonyl *trans* to the hydride on the osmium atom σ-bound to the carbon of the imidoyl ligand and the resonance at 174.11 to the carbonyl *cis* to the hydride on the same osmium atom. At 233 K we also observe three less intense off-diagonal elements between the resonances at 177.43, 170.03, and 168.88 ppm. These off-diagonal elements must arise from the onset of axial–radial exchange between the carbonyl groups on the nitrogen-bound osmium atom, and with the carbon hydrogen coupling and chemical shift information given

(24) Rosenberg, E.; Gobetto, R.; Aime, S.; Padovan, F.; Botta, M.; Gellert, R. *Organometallics* **1987**, *6*, 2074.

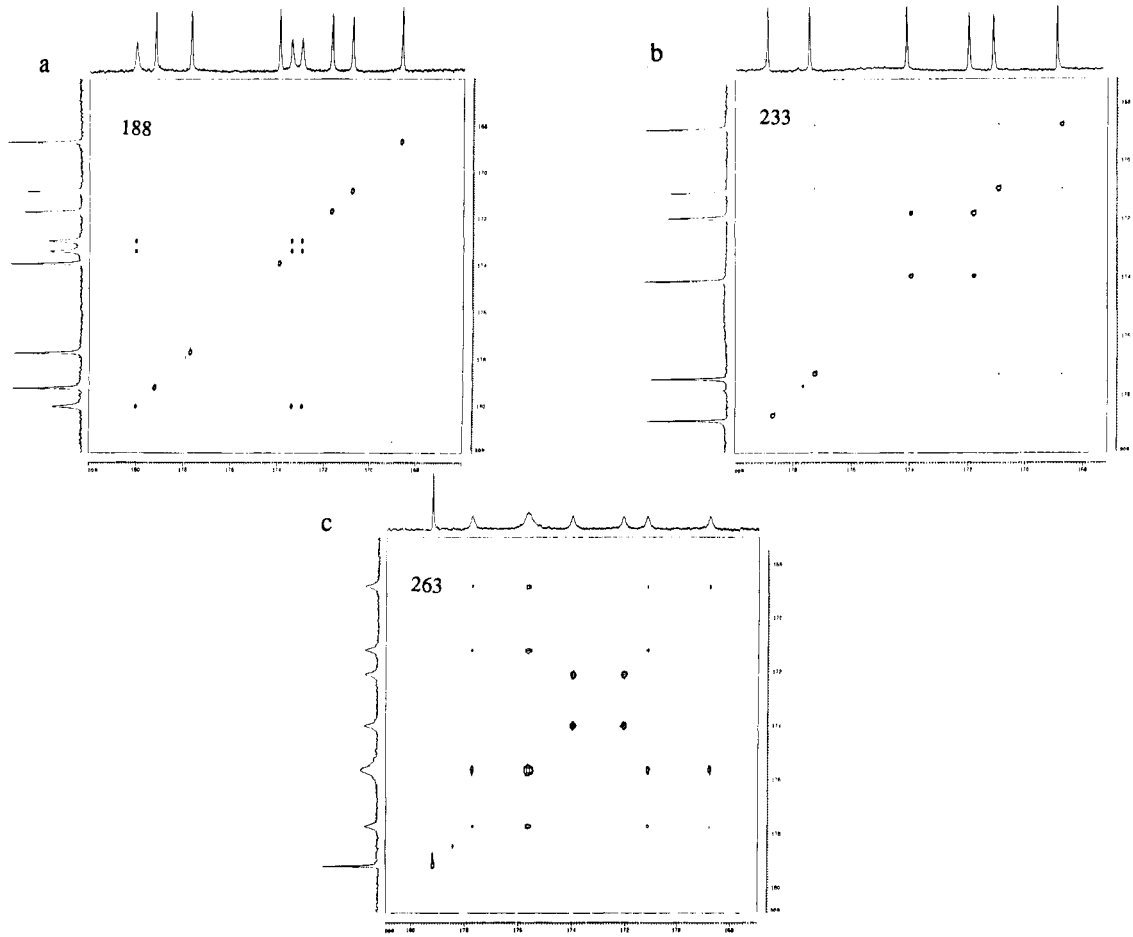

Figure 8. 2D-^{13}C-EXSY spectra at 90 MHz of **2** in CD_2Cl: (a) at 188 K, mixing time = 0.5 s; (b) at 233 K, mixing time = 0.5 s; (c) at 263 K, mixing time = 0.5 s.

above we can definitively assign the resonance at 170.03 ppm to the carbonyl *trans* to the hydride on the nitrogen-bound osmium atom, the resonance at 168.88 ppm to the radial carbonyl *cis* to the hydride on the same osmium atom, and the resonances at 177.43 to the axial carbonyl group on this osmium atom. It is significant that the three off-diagonal elements between the carbonyl groups on the nitrogen-bound osmium atom are much less intense than those between the two radial carbonyls on the carbon-bound osmium atom, as this indicates that the windshield wiper motion is slightly faster than axial–radial exchange at the nitrogen-bound osmium atom. At 263 K we observe off-diagonal elements between the three carbonyl groups and the averaged resonance of the three carbonyl groups on the π-bound osmium atom at 175.2 ppm as well as an increase in the intensity of off-diagonal elements referred to above (Figure 8c). Here again, the more intense off-diagonal elements are those arising from magnetization transfer as a result of the windshield wiper motion. Significantly, the resonance at 178.88 ppm still shows no off-diagonal elements, indicating that the windshield wiper motion and the accompanying hydride edge hopping are not associated with axial–radial carbonyl exchange at the carbon-bound osmium. Thus the ^{13}C-EXSY spectra of **2** in combination with the one-dimensional ^{13}C-NMR data result in unambiguous assignment of all of the carbonyl group resonances (as shown in Figure 7, with the exception of the equivocal assignment of the radial carbonyls on the π-bound osmium atom) and a qualitative assessment of the relative rates of each stage of the fluxional process in **2**.

The complexes **16–19** all give VT-^{1}H-NMR spectra which reveal the presence of one major along with four–eight other minor isomers at 223 K, as indicated from the hydride resonances (Figures 9–12). The spectra of all four compounds in the hydride region share the common feature that one hydride resonance appears to remain sharp from 223 to 295 K. Thus for **16** five hydride resonances at −17.66, 17.99, −18.00, −18.50, and −18.96 ppm (relative intensity = 0.18, 0.08, 0.12, 0.07, 0.55) are observed in $CDCl_3$ (Figure 9). At 295 K all the resonances appear broadened into the baseline except for the one at −17.66 ppm, which remains sharp through this temperature range. A separate sample of **16** was examined in toluene-d_8 in the temperature range 233–363 K (Figure 10). Minor changes in population and chemical shift are noted with five hydride resonances at −17.53, −17.74, −17.88, −18.32, and −18.73 ppm (relative intensity = 0.21, 0.06, 0.18, 0.06, 0.49) being observed at 233 K. At 363 K we observed a broad resonance at −18.28 ppm, which is roughly the weighted average of the three resonances at −17.74, −17.88, and −18.73 ppm, with a shoulder which is the broadened −18.32 ppm resonance. The resonance at −17.53 ppm shows some broadening at this temperature. Similarly, **17** shows five hydride resonances at 223 K at −17.75, −18.10, −18.16, −18.52, and −19.14 ppm (relative intensity = 0.27, 0.05, 0.20, 0.07, 0.41). The resonance at −17.75 ppm remains sharp up to 333 K while the other four resonances broaden in this temperature range, but the resonance at −18.52 ppm appears to broaden less and then sharpen again at 333 K at a slightly lower chemical shift (−18.48 ppm) and overlaps with a broader resonance which is the weighted average of the

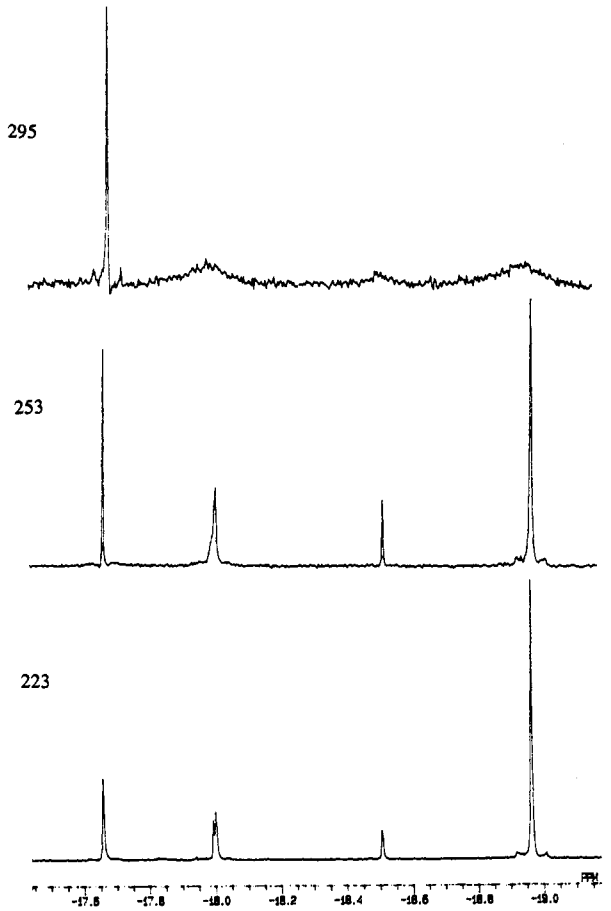

Figure 9. VT-^{1}H-NMR of **16** at 400 MHz in $CDCl_3$.

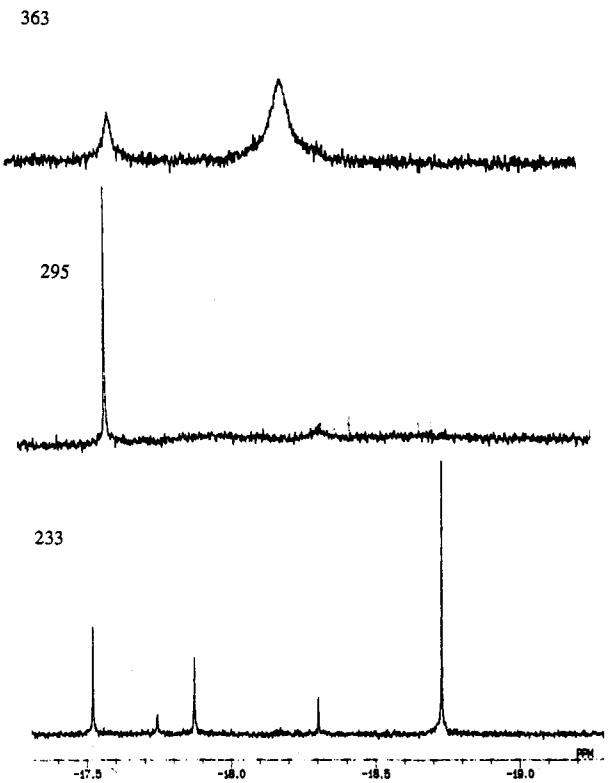

Figure 10. VT-^{1}H-NMR of **16** at 400 MHz in toluene-d_8.

resonances at −18.10, −18.16, and −19.14 ppm (Figure 11). Compound **18** shows nine hydride resonances at 223 K at −15.80, −16.29, −16.57, −17.34, −17.50, −17.62, −17.68, −18.11, and −18.53 ppm (relative intensity = 0.02, 0.06, 0.03, 0.14,

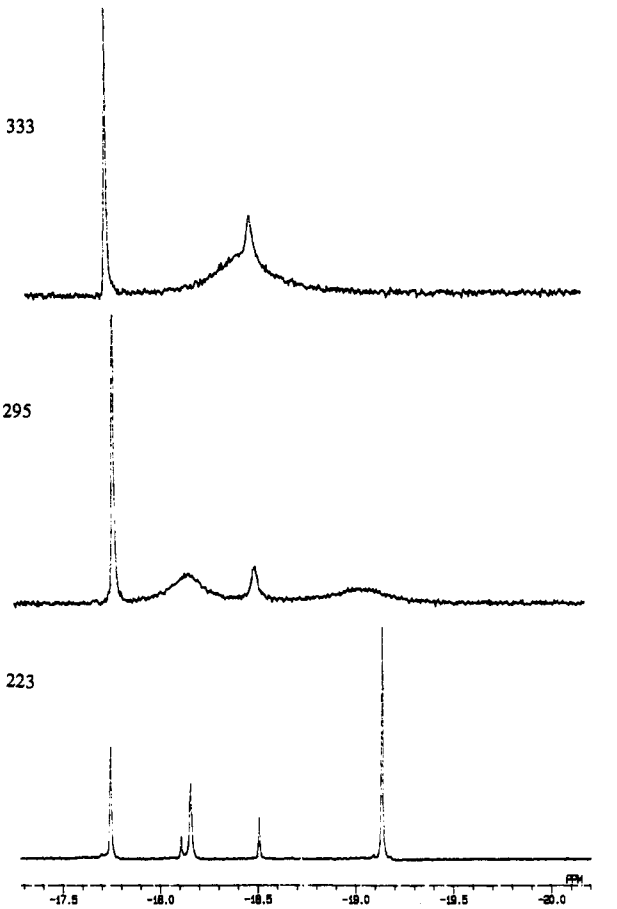

Figure 11. VT-^{1}H-NMR of **17** at 400 MHz in $CDCl_3$.

0.03, 0.04, 0.11, 0.03, 0.53). The overall behavior of **18** is similar to that of **16** and **17** as the temperature is increased, with the resonance of −17.34 ppm remaining sharp throughout the temperature range examined and the remaining resonances broadening and then coalescing to a broad resonance at −17.80 ppm, overlapping with a sharper resonance at −18.04 ppm (Figure 12). The VT-^{1}H-NMR of **19** is remarkably similar to that of **18** except only eight isomers are detected at −16.31, −16.48, −17.28, −17.39, −17.75, −17.80, −18.01, and −18.65 ppm (relative intensity = 0.07, 0.01, 0.04, 0.13, 0.06, 0.14, 0.06, 0.49) at 233 K. The resonance at −17.39 ppm remains sharp throughout the temperature range examined. The resonance at −18.01 broadens and resharpens with a slight downfield shift, while the remaining resonances are broadened into the baseline at 295 K.

It is not possible to fully understand the VT-^{1}H-NMR of **16**–**19** from the one-dimensional data alone. We therefore examined the 2D-^{1}H-EXSY spectra of **17**–**19**. Since we observe rapid broadening of the minor isomers just above the low temperature limit we decided to examine the ^{1}H-EXSY spectra of **18** near the low temperature limit but using different mixing times. Using a mixing time of 0.2 s, we observe off-diagonal elements between the major isomer at −18.53 ppm and two minor isomers at −17.50 and −16.29 ppm (Figure 13a). We also observe off-diagonal elements between the resonances at −16.57 and −17.62 ppm. If we assume that the major isomer found in solution is the same as that found in the solid state, the most straightforward explanation for these off-diagonal elements is the onset of axial–radial exchange between the major isomer (with the isonitrile ligand *trans* to the hydride on the osmium atom bound to nitrogen), the other radial

Figure 12. VT-^{1}H-NMR of 18 at 360 MHz in $CDCl_3$.

isomer (*cis* to the hydride), and the axial isomer on that same osmium atom. The off-diagonal elements between the resonances at −16.57 and −17.62 ppm suggest the onset of axial–radial exchange between two isomers with the isonitrile substituted at the π-bound osmium atom. It thus appears that in 18 tripodal motion at the nitrogen-bound osmium atom is of comparable rate to that of tripodal motion at the π-bound osmium atom, unlike 2 where the latter is much faster. Substitution for carbonyl at a metal atom in polynuclear complexes with phosphine[25] or isonitrile[26] has been shown to lower the barrier to axial–radial exchange but not in all cases and not always to the same degree. At mixing times of 0.5 s the off-diagonal elements referred to above intensify but no additional ones are observed. At mixing times of 1 s, however, we observe off-diagonal elements which indicate exchange between the two initially exchanging groups of isomers (Figure 13b). This is undoubtedly due to the onset of the windshield wiper motion and the associated hydride edge hopping. We also observe an additional off-diagonal element which

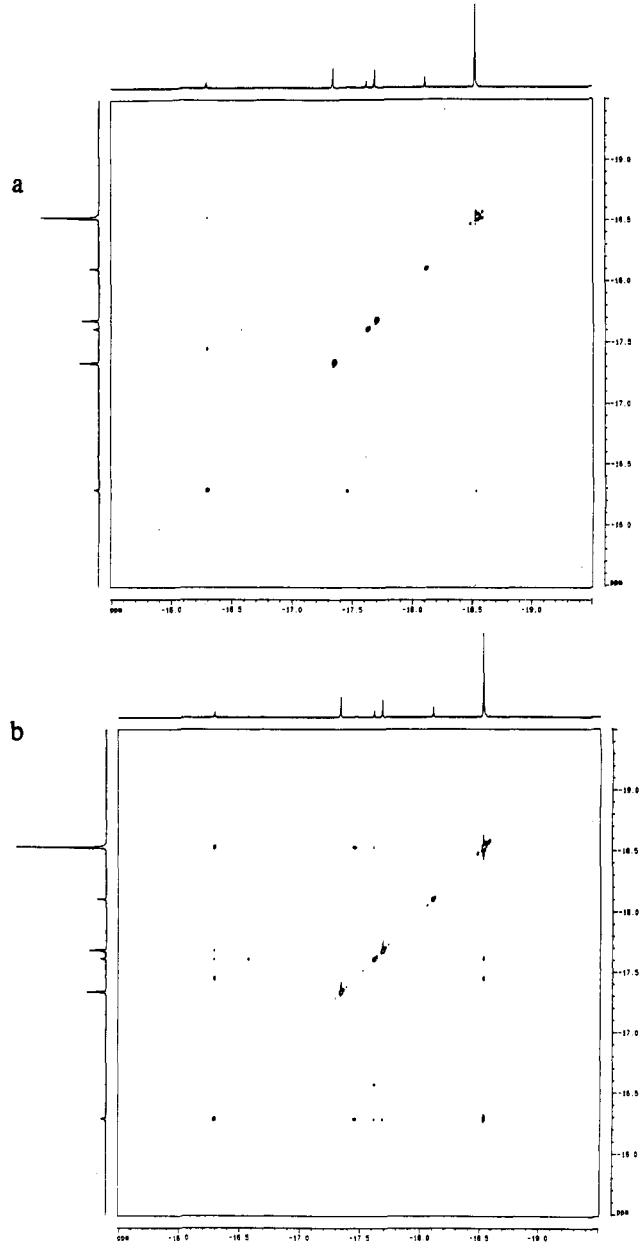

Figure 13. 2D-^{1}H-EXSY of 18 at 360 MHz in $CDCl_3$ at 233 K: (a) mixing time = 0.2 s; (b) mixing time = 1.0 s.

involves the resonance at −17.68 ppm in the exchange process but was not involved in the initial tripodal motions. We ascribe this isomer to structure A or B where the

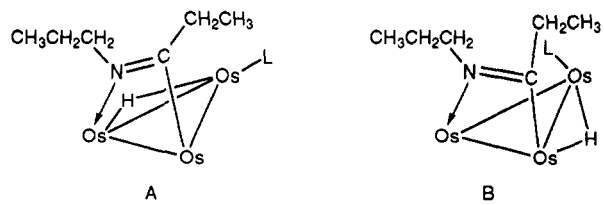

hydride and the μ-imidoyl are on different edges. An analog of this type of complex exists as the major isomer in solution and in the solid state for $(\mu\text{-H})Os_3(CO)_9(\mu\text{-}\eta^2\text{-}CH_3CH_2C{=}NCH_2CH_2CH_3)P(C_6H_5)_3$ (eq 4).[2] No off-diagonal elements are observed for the resonances at −17.34 and −18.11 ppm. The resonance at −17.34 shows no broadening throughout the temperature range examined, while the one at −18.11 shows slight broadening between −50 and +10 °C and then narrowing above +10 °C. We

(25) Jangala, C.; Rosenberg, E.; Skinner, D.; Aime, S.; Milone, L.; Sappa, E. *Inorg. Chem.* **1980**, *19*, 1571.
(26) (a) Farrugia, L. J. *Organometallics* **1989**, *8*, 2410. (b) Farrugia, L. J.; Rae, S. E. *Organometallics* **1991**, *10*, 3919.

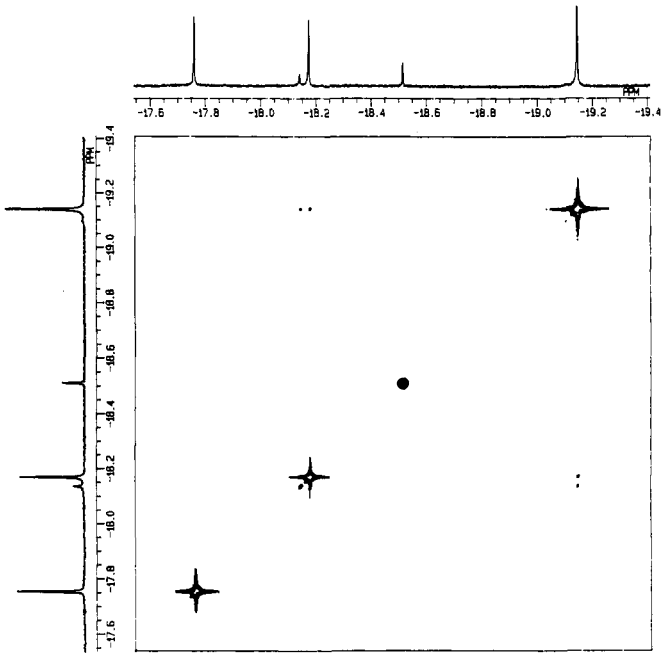

Figure 14. 2D-^{1}H-EXSY of 17 at 400 MHz in $CDCl_3$ at 233 K; mixing time = 1.0 s.

know from our ^{13}C-NMR studies of 2 that no axial–radial exchange of carbonyl groups occurs at the osmium atom σ-bound to the carbon atom up to +23 °C. Extrapolating this observation to 18, we can assign the resonance at −17.34 ppm to an isomer in which the isocyanide ligand is in an axial position on the osmium atom σ-bound to the carbon atom of the imidoyl ligand and the resonance at −18.11 ppm to an isomer in which the isocyanide ligand is in a radial position on the same osmium atom presumably *trans* to the hydride as in the major isomer. The windshield wiper–edge hopping of the hydride would exchange this isomer with the other radial isomer (where the isocyanide ligand is *cis* to hydride ligand on the osmium atom σ-bound to the carbon atom). The slight broadening of this resonance is undoubtedly due to averaging with an undetectable amount of this minor isomer (or the very minor isomer detected at −15.80 ppm). The ^{1}H-EXSY spectra of 19 at 0.5- and 1.0-s mixing times shows off-diagonal element patterns exactly analogous to those of 18. In the case of 17 where only five isomers are detected in the ^{1}H-NMR at −50 °C (Figure 11) the ^{1}H-EXSY spectra at mixing times of 0.5 and 1.0 s show off-diagonal elements between only three resonances, the major isomer at −19.14 ppm and two minor isomers at −18.10 and −18.16 ppm (Figure 14). Using the information gained from the ^{1}H-EXSY spectra of 18, we conclude that we are observing axial–radial exchange at the nitrogen-bound osmium atom. The resonance at −17.66 ppm remains sharp from −50 to +23 °C, while the one at −18.50 ppm shows broadening and renarrowing in this temperature range along with a slight downfield shift. We therefore assign these resonances to axial and radial isomers with the isocyanide ligand on the carbon-bound osmium atom. Apparently, with the less sterically demanding imidoyl ligand in 16 and 17 we do not observe a significant population of the isomers with the isocyanide ligand at the π-bound osmium atom. The overall dynamic behavior of 16–19 appears to be the same as that of 2 with the notable difference that axial–radial exchange at the nitrogen-bound osmium atom is significantly faster than in 2. It is not obvious why this should be the case, especially in light of the fact that the phosphine analogs of 16–19 are rigid on the NMR time scale at room temperature at the nitrogen-bound osmium atom.[2] These results have caused us to reevaluate an earlier generalization about ligand dynamics in hydrido carbonyl clusters which stated that axial–radial exchange at hydride-bridged metal atoms is always slower than at the nonbridged metal atoms in a cluster.[27] This pattern seems to hold for 2 and the phosphine derivatives of 2 but not for 16–19. Finally, at temperatures of 60–90 °C we observe the beginning of what appears to be the complete averaging of all the isomers in 16 (Figure 10), suggesting axial–radial exchange at all three metal centers along with imidoyl ligand rotation.

The dynamic behavior of 16–19 is summarized in Scheme III. There are overall two sets of isomers. One set a–c and their enantiomers d–f are interchanged by the windshield wiper motion with a rate constant k_2, which is much faster for this set of isomers than k_1, the rate for tripodal rotation at the osmium σ-bound to the carbon of the imidoyl ligand. Only two of these three isomers and their enantiomers are detected, with one pair definitely being c and e. In the other set of isomers g–n, isomers l (major isomer), m, and n and i, j, and k are first interchanged by tripodal rotation with rate constants k_3 and k_4, which are comparable in magnitude, and interchange between these subsets occurs with a rate constant k_5, which is smaller than k_3 and k_4. Only two of isomer set i, j, and k are detected for 18 and 19, while none of this set is observed for 16 and 17. In the case of 18 or 19 an additional isomer is detected which interchanges with i–n by hydride edge hopping and to which we assign structure g or h. The rate constants k_6 and k_7 are apparently similar in magnitude to k_5. The ninth low intensity isomer detected for 18 (at −15.80 ppm) cannot be correlated with a specific set since it did not show up on the diagonal or give an off-diagonal element.

Experimental Section

General Procedures. Although the reaction products are air stable, all the reactions were performed under an atmosphere of nitrogen, unless stated otherwise. Methylene chloride and acetonitrile were distilled from calcium hydride, and benzene and hexane, from sodium benzophenone ketyl prior to use. Pyrrolidine and di-*n*-propylamine were purchased from Aldrich and distilled from sodium directly before use after predrying with potassium hydroxide. Methyl isocyanide was prepared according to the known procedures[28] and freshly distilled prior to use. *tert*-Butyl isocyanide was purchased from Aldrich and used as received. $Os_3(CO)_{10}(CH_3CN)_2$,[29] $Os_3(CO)_{11}(CH_3CN)$,[29] and $(\mu\text{-H})Os_3(CO)_{10}(\mu\text{-}\eta^2\text{-}CHCH_2)$[16] were prepared according to the published procedures. IR spectra were recorded on a Perkin-Elmer 1420 spectrophotometer. ^{1}H-NMR spectra were obtained on an IBM-NR80, Bruker-AM400, Bruker AMX360, or a JEOL-GX400 spectrometer. Two-dimensional ^{1}H and ^{13}C phase sensitive EXSY spectra were obtained using the Bruker pulse program NOESY-TPPI or the JEOL program VNOENH with relaxation delays of 2 s using 8–16 scans. Elemental analyses were performed by Schwarzkopf Microanalytical Laboratory (New York, NY). Photochemical reactions were carried out using a Rayonet photochemical reactor irradiating with 3000-Å lamps.

(27) Aime, S.; Gobetto, R.; Osella, D.; Milone, L.; Rosenberg, E. *Organometallics* **1982**, *1*, 640.
(28) Schuster, R. E.; Scott, J. E.; Cassanova, J., Jr. *Organic Syntheses*; Wiley: New York, 1973, Collect. Vol. 5, p 772.
(29) Johnson, B. F. G.; Lewis, J.; Pippard, D. A. *J. Chem. Soc., Dalton Trans.* **1981**, 407.

Scheme III

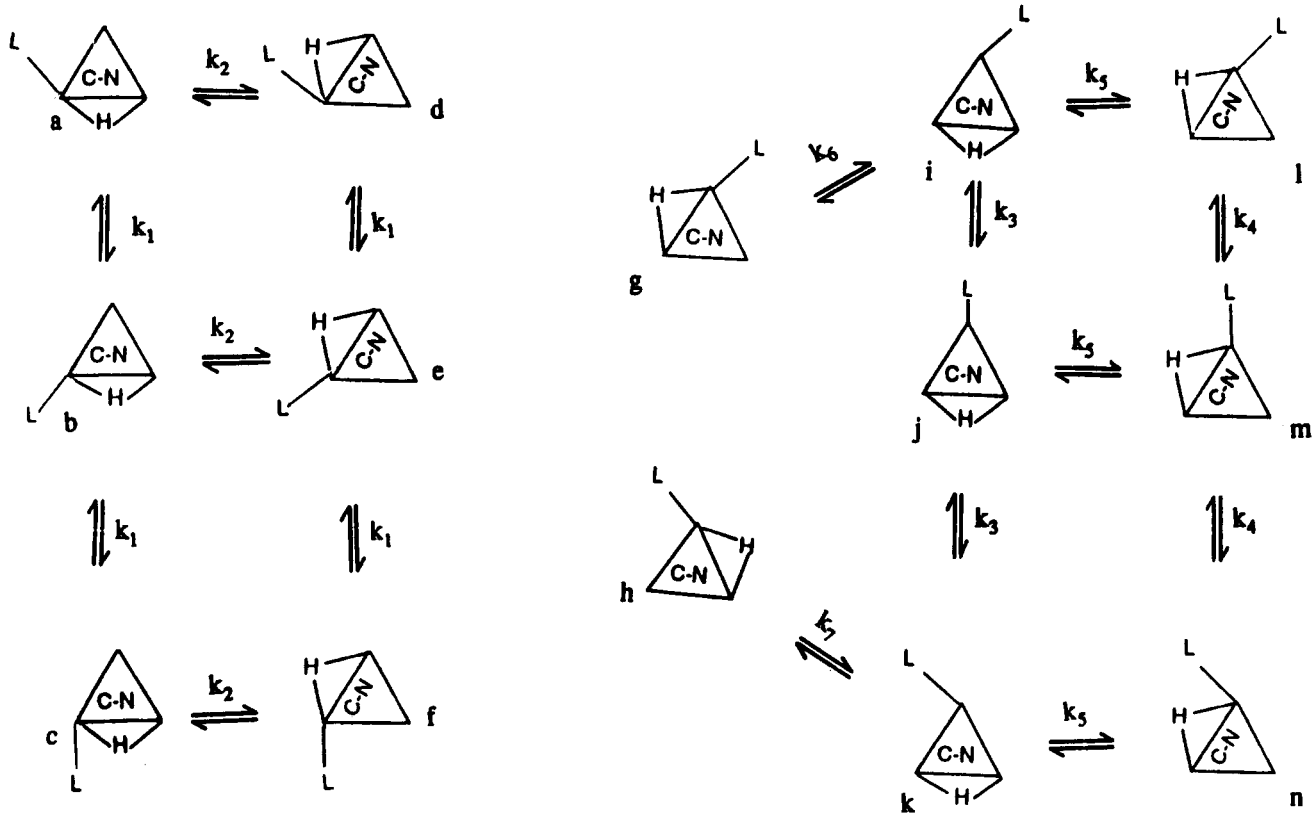

Reaction of $Os_3(CO)_{10}(CH_3CN)_2$ (1) with Pyrrolidine: Synthesis of $(\mu\text{-H})(\mu\text{-}\eta^1\text{-NCH}_2\text{CH}_2\text{CH}_2\text{CH}_2)Os_3(CO)_{10}$ (9) and $(\mu\text{-H})(\mu\text{-}\eta^2\text{C=NCH}_2\text{CH}_2\text{CH}_2)Os_3(CO)_{10}$ (10). Pyrrolidine (179 μL, 2.14 mmol) was added to a freshly distilled benzene solution (200 mL) of 1 (0.400 g, 0.429 mmol) in a 500-mL three-necked round bottom flask equipped with a magnetic stirring bar, a reflux condenser topped with a stopcock connected to an oil bubbler, and an inlet tube for bubbling nitrogen into the solution. The color turned to orange immediately after the addition of pyrrolidine. The reaction mixture was heated at 40–45 °C for 8 h while nitrogen were bubbled through the solution. The solvent was removed under vacuum. The residue was dissolved in a minimum volume of CH_2Cl_2 and chromatographed by TLC on silica gel. Elution with a hexane/CH_2Cl_2 (10:1, v/v) mixture gave three main bands from which the following compounds were isolated (in order of elution): purple band, $(\mu\text{-H})_2Os_3(CO)_{10}$ (0.015 g, 4%); orange band, **9** (0.028 g, 7%) as orange-red crystals after recrystallization from hexane/CH_2Cl_2 at −20 °C; yellow band, **10** (0.197 g, 50%) as yellow crystals after recrystallization from hexane/CH_2Cl_2 at −20 °C.

Spectral and analytical data for 9: IR (ν(CO) in cyclohexane) 2099 (w), 2057 (vs), 2046 (s), 2015 (vs), 2002 (s), 1982 (s), 1972 (w) cm^{-1}; 80-MHz ^{1}H-NMR (in $CDCl_3$) 3.84 (t, 2 H, J_{H-H} = 7.2 Hz), 3.26 (t, 2H, J_{H-H} = 7.2 Hz), 1.84 (m, 4H), −13.69 (s, 1H) ppm. Anal. Calcd for $C_{14}H_9NO_{10}Os_3$: C, 18.24; H, 0.99; N, 1.52. Found: C, 18.45; H, 0.92; N, 1.60.

Spectral and analytical data for 10: IR (ν(CO) in cyclohexane) 2102 (m), 2060 (vs), 2048 (s), 2021 (s), 2002 (vs), 1998 (sh), 1988 (s), 1974 (w) cm^{-1}; 80-MHz ^{1}H-NMR (in $CDCl_3$) 3.57 (m, 2H), 2.46 (m, 2H), 1.77 (m, 2H), −15.33 (s, 1H) ppm. Anal. Calcd for $C_{14}H_7NO_{10}Os_3$: C, 18.28; H, 0.77; N, 1.52. Found: C, 18.40; H, 0.58; N, 1.58.

Decarbonylation of 10: Synthesis of $(\mu\text{-H})(\mu_3\text{-}\eta^2\text{-C=NCH}_2\text{CH}_2\text{CH}_2)Os_3(CO)_9$ (2). (a) Thermal Route. The cluster **10** (0.174 g, 0.190 mmol) was dissolved in octane (40 mL) in a 200-mL Schlenk tube. The solution was vigorously refluxed for 24 h. The color changed from yellow to pale yellow. The solvent was removed under pressure, and the residue was chromatographed by TLC on silica gel. Elution with hexane/CH_2Cl_2 (10:3 v/v) gave two bands. The fastest moving band gave unconsumed **10** (0.010 g). The slowest moving band gave **2** (0.153 g, 90% based on the amount **10** consumed).

Spectral and analytical data for 2: IR (ν(CO) in cyclohexane) 2089 (m), 2063 (vs), 2036 (vs), 2011 (vs), 1998 (m), 1990 (s), 1978 (sh), 1964 (w) cm^{-1}; 400-MHz ^{1}H-NMR (in CD_2Cl_2 at −40 °C (low-temperature limit)) 3.46 (two multiplets partially overlapping, 2H), 3.10 (m, 1H), 2.97 (m, 1H), 2.10 (m, 1H), 1.59 (m, 1H), −17.96 (s, 1H); 400-MHz ^{1}H-NMR (in CD_2Cl_2 at +40 °C (high-temperature limit)) 3.46 (t, 2H, J_{H-H} = 6.9 Hz), 3.05 (t, 2H, J_{H-H} = 6.8 Hz), 1.85 (t, 2H, J_{H-H} = 6.4 Hz), −17.96 (s, 1 H). Anal. Calcd for $C_{13}H_7NO_9Os_3$: C, 17.51; H, 0.79; N, 1.57. Found: C, 17.71; H, 0.71; N, 1.64.

(b) Photochemical Route. A solution of compound **10** (0.160 g, 0.179 mmol) in hexane (150 mL) was irradiated for 1.5 h. The solvent was removed under vacuum, and the residue was chromatographed by TLC on silica gel. Elution with hexane/CH_2Cl_2 (10:3, v/v) resolved three bands. The faster moving band gave unconsumed **10** (0.008 g). The second band yielded **2** (0.140 g, 90%). The slowest moving band gave too small an amount for further characterization.

Conversion of 9 to 10. A heptane solution (20 mL) of **9** (0.015 g, 0.016 mmol) was refluxed for 4 h under nitrogen. The color changed from orange to yellow. The conversion appeared to be quantitative by analytical TLC. The solvent was removed under vacuum and the residue was applied to silica gel TLC plates. Elution with hexane/CH_2Cl_2 (10:1, v/v) gave a single band which yielded **10** (0.014 g, 93%).

Reaction of 1 with Di-*n*-propylamine: Synthesis of $(\mu\text{-H})(\mu\text{-}\eta^2\text{-CH}_3\text{CH}_2\text{C=NCH}_2\text{CH}_2\text{CH}_3)Os_3(CO)_{10}$ (11). (a) At Room Temperature. To a dichloromethane solution (40 mL) of **1** (0.224 g, 0240 mmol) was added a 5-fold molar excess of $(CH_3CH_2CH_2)_2NH$ (167 μL, 1.20 mmol). The resulting mixture was stirred for 24 h at room temperature. The solvent and the excess di-*n*-propylamine were removed under reduced pressure, and the residue was chromatographed on silica gel TLC plates. Elution with hexane/CH_2Cl_2 (10:2 v/v) gave four bands from which

the following compounds were isolated (in order of elution): (μ-H)$_2$Os$_3$(CO)$_{10}$ (0.004 g, 2%); Os$_3$(CO)$_{12}$ (0.004 g, 2%); (μ-H)(μ-η^2-CH$_3$CH$_2$C=NCH$_2$CH$_2$CH$_3$)Os$_3$(CO)$_{10}$ (11) (0.080 g, 35%) as yellow crystals after recrystallization from hexane/CH_2Cl_2 at −20 °C; (μ-H)(μ-OH)Os$_3$(CO)$_{10}$ (0.020 g, 10%).

Spectral and analytical data for 11: IR (ν(CO) in hexane) 2100 (m), 2057 (vs), 2047 (s), 2020 (s), 2001 (vs), 1998 (sh), 1983 (s), 1970 (w) cm^{-1}; 80-MHz ^{1}H-NMR (in C_6D_6) 3.24 (m, 1H), 2.78 (m, 1H), 2.13 (m, 2H), 1.17 (m, 2H), 0.73 (t, 3H, J_{H-H} = 7.6 Hz), 0.45 (t, 3H, J_{H-H} = 7.3 Hz), −15.19 (s, 1H). Anal. Calcd for $C_{16}H_{13}NO_{10}Os_3$: C, 20.23; H, 1.38; N, 1.48. Found: C, 20.44; H, 1.26; N, 1.54.

(b) At 40–50 °C. *Into* a three-necked round bottom flask equipped with a magnetic stirring bar, a gas inlet tube for bubbling nitrogen into the solution, a gas outlet, and a reflux condenser were combined 1 (0.400 g, 0.429 mmol), di-*n*-propylamine (199 μL, 1.43 mmol), and benzene (200 mL). The resulting mixture was heated at 40–50 °C for 8 h while nitrogen was bubbled through it. Workup as described above followed by similar chromatographic separation gave, in order of elution, (μ-H)$_2$Os$_3$(CO)$_{10}$ (0.007 g, 2%), Os$_3$(CO)$_{12}$ (0.004 g, 1%), (μ-H)(μ-η^2-CH$_2$CH$_2$C=NCH$_2$CH$_2$CH$_3$)Os$_3$(CO)$_{10}$ (11, 0.179 g, 44%), and (μ-H)(μ-OH)Os$_3$(CO)$_{10}$ (0.023 g, 6%).

Reaction of (μ-H)(μ-η^2-CHCH$_2$)Os$_3$(CO)$_{10}$ with Di-*n*-propylamine: Synthesis of 11. Into a 250-mL three-necked round bottom flask were combined (μ-H)(μ-η^2-CHCH$_2$)Os$_3$(CO)$_{10}$ (0.353 g, 0.402 mmol) di-*n*-propylamine (278 μL, 2.01 mmol), and benzene (100 mL). The reaction mixture was refluxed for 8 h. The solvent was evaporated to dryness. Chromatographic separation of the residue as described above gave two bands which yielded the following compounds (in order of elution): (μ-H)$_2$Os$_3$(CO)$_{10}$ (0.010 g, 3%); 11 (0.160 g, 42%).

Decarbonylation of 11: Synthesis of (μ-H)(μ_3-η^2-CH$_3$CH$_2$C=NCH$_2$CH$_2$CH$_3$)Os$_3$(CO)$_9$ (3). (a) Thermal Route. An octane solution (40 mL) of 11 (0.163 g, 0.172 mmol) was refluxed vigorously for 24 h. The solution turned from yellow to pale yellow. The solvent was removed in vacuo, and the residue was chromatographed by TLC on silica gel. Elution with hexane/CH_2Cl_2 resolved three bands. The fastest moving band gave unreacted 11 (0.003 g). The second band gave Os$_3$(CO)$_{12}$ (0.003 g, 2%). The main band gave (μ-H)(μ_3-η^2-CH$_3$CH$_2$C=NCH$_2$CH$_2$CH$_3$)Os$_3$(CO)$_9$ (3) (0.146 g, 92%) as pale yellow crystals after recrystallization from hexane/CH_2Cl_2 at −20 °C.

Spectral and analytical data for 3: IR (ν(CO) in cyclohexane) 2087 (m), 2059 (vs), 2035 (vs), 2008 (vs), 1994 (m), 1986 (s), 1977 (sh), 1963 (w) cm^{-1}; 400-MHz ^{1}H-NMR (in CD_2Cl_2 at −49 °C (low-temperature limit)) 3.91 (m, 1H), 2.94 (two partially overlapping multiplets, 2H), 2.65 (m, 1H), 1.75 (m, 1H), 1.43 (m, 1H), 1.15 (t, 3H, J_{H-H} = 7.4 Hz), 0.86 (t, 3H, J_{H-H} = 7.4 Hz), −17.54 (s, 1H) ppm. Anal. Calcd for $C_{15}H_{13}NO_9Os_3$: C, 19.54; H, 1.43; N, 1.52. Found: C, 19.59; H, 1.30; N, 1.58.

(b) Photochemical Route. A hexane solution (100 mL) of 11 (0.130 g, 0.137 mmol) in a 200-mL quartz tube was irradiated for 1 h. The color changed from yellow to pale yellow. The solvent was removed under vacuum and the residue was chromatographed as above to give unconsumed 11 (0.002 g), Os$_3$(CO)$_{12}$ (0.005 g, 4%), and 3 (0.117 g, 93%).

Reaction of 2 with Methyl Isocyanide. To a freshly distilled hexane solution (30 mL) of 2 (0.068 g, 0076 mmol) was added methyl isocyanide (6 μL, 0.088 mmol). Immediate formation of a yellow precipitate was observed. Analytical TLC showed total consumption of 2. The solvent and excess methyl isocyanide were removed by blowing nitrogen, and the residue was washed with cold hexane. The yellow solid thus obtained was recrystallized from hexane/CH_2Cl_2 at −20 °C to give (μ-H)(μ-η^2-C=NCH$_2$CH$_2$CH$_2$)Os$_3$(CO)$_9$(CNCH$_3$) (12). IR (in hexane): ν(CO) 2076 (w), 2045 (vs), 2026 (vs), 1999 (w), 1980 (s, br), 1956 (w) cm^{-1}; ν(CN) 2205 cm^{-1}. ^{1}H-NMR (400 MHz) (in CD_2Cl_2): major isomer (81%) 3.66 (s, 3H), 3.51 (two multiplets partially overlapping, 2H) 2.39 (m, 2H), 1.66 (m, 2H), −14.68 (s, 1H) ppm. Anal. Calcd for $C_{15}H_{10}N_2O_9Os_3$: C, 19.31; H, 1.08; N, 3.0. Found: C, 19.51; H, 1.20; N, 3.11.

Reaction of 2 with *tert*-Butyl Isocyanide. To a pale yellow hexane solution (60 mL) of 2 (0.100 g, 0.112 mmol) was added *tert*-butyl isocyanide (26 μL, 0.229 mmol). The color immediately changed to bright yellow. After stirring for 1 h at room temperature, analytical TLC showed complete consumption of 2 with the formation of a single product. The volatiles were removed by blowing nitrogen through the solution. The residue was chromatographed by TLC on silica gel. Elution with hexane/CH_2Cl_2 (10:3, v/v) gave a single band which yielded (μ-H)(μ-η^2-C=NCH$_2$CH$_2$CH$_2$)Os$_3$(CO)$_9$(CNC(CH$_3$)$_3$) (13) as yellow crystals (0.102 g, 92%) after recrystallization from hexane/CH_2Cl_2 at −20 °C.

Spectral and analytical data for 13: IR (in hexane) ν(CO) 2066 (w), 2045 (vs), 2024 (vs), 1998 (w), 1979 (vs), 1975 (vs, sh), 1954 (w) cm^{-1}; IR (in hexane) ν(CN) 2174 cm^{-1}; 400-MHz ^{1}H-NMR (in $CDCl_3$) major isomer (88%) 3.50 (m, 2H), 2.37 (m, 2H), 1.70 (m, 2H), 1.40 (s, 9H), −14.89 (s, 1H) ppm. Anal. Calcd for $C_{18}H_{16}N_2O_9Os_3$: C, 22.17; H, 1.66; N, 2.87. Found: C, 22.19; H, 1.55; N, 2.88.

Reaction of 3 with Methyl Isocyanide. Methyl isocyanide (6 μL, 0.122 mmol) was added to a hexane solution (20 mL) of the cluster 3 (0.062 g, 0.067 mmol). The pale yellow solution of 3 turned dark yellow immediately after the addition of methyl isocyanide. The solution was stirred at room temperature for 1 h. The solvent was removed in vacuo, and the residue was chromatographed by TLC on silica gel. Elution with hexane/CH_2Cl_2 (10:2, v/v) gave two bands. The fastest moving band gave a small quantity (~0.001 g) of an uncharacterized compound. The second band gave (μ-H)(μ-η^2-CH$_3$CH$_2$C=NCH$_2$CH$_2$CH$_3$)Os$_3$(CO)$_9$(CNCH$_3$) (14) as yellow crystals (0.056 g, 86%) after recrystallization from hexane/CH_2Cl_2 at −20 °C.

Spectral and analytical data for 14: IR (in hexane) ν(CO) 2082 (w), 2065 (w), 2042 (vs), 2026 (vs), 1998 (w), 1979 (s), 1972 (s), 1954 (w) cm^{-1}; IR (in hexane) ν(CN) 2205 cm^{-1}; 400-MHz ^{1}H-NMR (in CD_2Cl_2) major isomer (72%) 3.63 (s, 3H), 3.62 (m, 1H) 3.11 (m, 1H), 2.63 (m, 1H), 2.26 (m, 1H), 1.63 (m, 1H), 1.40 (m, 1H), 1.01 (t, 3H, J_{H-H} = 7.7 Hz), 0.86 (t, 3H, J_{H-H} = 7.6 Hz), −14.28 (s, 1H) ppm. Anal. Calcd for $C_{17}H_{16}N_2O_9Os_3$: C, 21.20; H, 1.68; N, 2.91. Found: C, 21.21, H, 1.68; N, 2.87.

Reaction of 3 with *tert*-Butyl Isocyanide. A reaction, similar to that above, of 3 (0.130 g, 0.141 mmol) with *tert*-butyl isocyanide (48 μL, 0.421 mmol) followed by similar chromatographic separation gave (μ-H)(μ-η^2-CH$_3$CH$_2$C=NCH$_2$CH$_2$CH$_3$)Os$_3$(CO)$_9$(CNC(CH$_3$)$_3$) (15) as yellow crystals (0.128 g, 90%) after recrystallization from hexane/CH_2Cl_2 at −20 °C.

Spectral and analytical data for 15: IR (in hexane) ν(CO) 2080 (w), 2075 (vs), 2043 (vs), 1998 (w), 1978 (s), 1970 (s), 1962 (w), 1952 (w) cm^{-1}; IR (in hexane) ν(CN) 2175 cm^{-1}; 400-MHz ^{1}H-NMR (in $CDCl_3$) major isomer (76%) 3.63 (m, 1H), 3.30 (m, 1H), 2.64 (m, 1H), 2.25 (m, 1H), 1.65 (m, 1H), 1.40 (s, 9H), 1.36 (m, 1H), 1.00 (t, 3H, J_{H-H} = 7.5 Hz), 0.85 (t, 3H, J_{H-H} = 7.5 Hz), −14.49 (s, 1H) ppm. Anal. Calcd for $C_{20}H_{22}N_2O_9Os_3$: C, 23.90; H, 2.21; N, 2.79. Found: C, 24.12; H, 2.30; N, 2.85.

Thermolysis of 12. The cluster 12 (0.050 g, 0.054 mmol) and octane (20 mL) were combined in a 100-mL three-necked round bottom flask. The solution was refluxed for 8 h while nitrogen were bubbled through it. After cooling, the solvent was rotary evaporated and the residue was chromatographed by TLC on silica plates. Elution with hexane/CH_2Cl_2 (10:3 v/v) gave four bands from which the following compounds were isolated (in order of elution): 10 (0.004 g, 8%); 2 (0.005 g, 10%); unconsumed 12 (0.005 g), (μ-H)(μ_3-η^2-C=NCH$_2$CH$_2$CH$_2$)Os$_3$(CO)$_9$(CNCH$_3$) (16) as pale yellow crystals (0.028 g, 58%) after recrystallization from hexane/CH_2Cl_2 at −20 °C.

Spectral and analytical data for 16: IR (in hexane) ν(CO) 2073 (s), 2052 (w), 2033 (vs), 2015 (vs), 2000 (s), 1992 (s), 1980 (s), 1969 (m), 1965 (m), 1950 (w) cm^{-1}; IR (in hexane) ν(CN) 2189 cm^{-1}; 400-MHz ^{1}H-NMR (in CD_2Cl_2 at −50 °C (low-temperature limit)) major isomer (64%) 3.63 (s, 3H), 3.33 (two multiplets

partially overlapping, 2H), 3.09 (m, 1H), 2.92 (m, 1H), 1.98 (m, 1H), 1.49 (m, 1H), −18.58 (s, 1H) ppm. Anal. Calcd for $C_{14}H_{10}N_2O_8Os_3$: C, 18.58; H, 1.12; N, 3.10. Found: C, 18.61; H, 0.99; N, 3.00.

Thermolysis of 13. A similar thermolysis of **13** (0.060 g, 0.062 mmol) in octane (40 mL) for 8 h followed by similar chromatographic separation gave **10** (0.003 g, 5%), **2** (0.003 g, 5%), unconsumed **13** (0.015 g), and (μ-H)(μ_3-η^2-C=$NCH_2CH_2CH_2$)-$Os_3(CO)_8(CNC(CH_3)_3)$ (**17**) as pale yellow crystals (0.030 g, 51%) after recrystallization from hexane/CH_2Cl_2 at −20 °C).

Spectral and analytical data for 17: IR (in hexane) ν(CO) 2075 (w), 2070 (s), 2029 (vs), 2010 (vs), 1997 (sh), 1991 (m), 1978 (m), 1965 (m), 1960 (m), 1954 (w) cm^{-1}; IR (in hexane) ν(CN) 2163 cm^{-1}; 400-MHz ^{1}H-NMR (in $CDCl_3$ at −50 °C (low-temperature limit)) major isomer (41%) 3.35 (two multiplets partially overlapping, 2H), 3.15 (m, 1H), 3.01 (m, 1H), 2.10 (m, 1H), 1.74 (m, 1H), 1.48 (s, 9H), −19.17 (s, 1H) ppm. Anal. Calcd for $C_{17}H_{18}N_2O_8Os_3$: C, 22.54; H, 1.69; N, 2.92. Found: C, 22.62; H, 1.55; N, 2.90.

Thermolysis of 14. A solution of compound **14** (0.040 g, 0.042 mmol) in octane (30 mL) in a Schlenk tube was refluxed for 12 h. The color changed from yellow to pale yellow. The solvent was removed in vacuo, and the residue was separated by TLC on silica gel. Elution with hexane/CH_2Cl_2 (10:3 v/v) gave four bands from which the following compounds were isolated (in order of elution): **11** (0.002 g, 5%); **3** (0.002 g, 5%); unconsumed **14** (0.001 g); (μ-H)(μ_3-η^2-CH_3CH_2C=$NCH_2CH_2CH_3$)$Os_3(CO)_8$-$(CNCH_3)$ (**18**) as pale yellow crystals (0.030 g, 77%) after recrystallization from hexane/CH_2Cl_2 at −20 °C.

Spectral and analytical data for 18: IR (in hexane) ν(CO) 2070 (s), 2048 (w), 2031 (vs), 2015 (sh), 2011 (vs), 1996 (s), 1989 (s), 1977 (s), 1967 (m), 1962 (sh), 1949 (m) cm^{-1}; IR (in hexane) ν(CN) 2188 cm^{-1}; 270-MHz ^{1}H-NMR (in $CDCl_3$ at −50 °C (low-temperature limit)) major isomer (56%) 3.87 (m, 1H), 3.74 (s, 3H), 3.00 (to multiplets partially overlapping, 2H), 2.71 (m, 1H), 1.75 (m, 1H), 1.46 (m, 1H), −18.50 (s, 1H) ppm. Anal. Calcd for $C_{16}H_{16}N_2O_8Os_3$: 20.55; H, 1.73; N, 3.00. Found: C, 20.79; H, 1.85; N, 3.10.

Thermolysis of 15. A similar thermolysis of **15** (0.085 g, 0.085 mmol) in octane (25 mL) for 8 h followed by similar chromatographic separation resolved four bands which gave (in order of elution) **11** (0.003 g, 3%), **3** (0.003 g, 3%), unconsumed **15** (0.005 g) and (μ-H(μ_3-η^2-CH_3CH_2C=$NCH_2CH_2CH_3$)$Os_3(CO)_8(CNC$-$(CH_3)_3)$ (**19**) as pale yellow crystals (0.066 g, 80%) after recrystallization from hexane/CH_2Cl_2 at −20 °C.

Spectral and analytical data for 19: IR (in hexane) ν(CO) 2069 (s), 2948 (w), 2929 (vs), 2013 (vs), 2008 (vs), 1995 (sh), 1990 (s), 1976 (s), 1965 (m), 1960 (m), 1948 (m) cm^{-1}; IR (in hexane) ν(CN) 2162 (w) cm^{-1}; 400-MHz ^{1}H-NMR (in $CDCl_3$ at −50 °C) (low-temperature limit) major isomer (46%) 3.86 (m, 1H), 2.96 (m, 1H), 2.72 (two multiplets partially overlapping, 2H), 1.75 (m, 1H), 1.62 (m, 1H), 1.38 (s, 9H), 1.14 (t, 3H, J_{H-H} = 7.3 Hz), 0.85 (t, 3H, J_{H-H} = 7.1 Hz), −18.68 (s 1H) ppm. Anal. Calcd for $C_{19}H_{22}N_2O_8Os_3$: C, 23.36; H, 2.27; N, 2.87. Found: C, 23.45; H, 2.15; N, 2.92.

X-ray Structure Determination of 2, 9, 12, 13, and 16. Crystals of **2, 9, 12, 13,** and **16** for X-ray examination were obtained from saturated solutions of each in dichloromethane/hexane solvent systems at −20 °C. Suitable crystals for each were mounted on glass fibers, placed in a goniometer head on an Enraf-Nonius CAD4 diffractometer, and centered optically. Until cell parameters and the orientation matrix for data collection were obtained using the centering program in the CAD4 system. Details of the crystal data are given in Table I. For each crystal the actual scan range was calculated by scan width − scan range + 0.35 tan θ and backgrounds were measured using the moving crystal–moving counter techniques at the beginning and end of each scan. As a check on instrument and crystal stability, two representative reflections for **2** and three reflections for **9, 12, 13,** and **16** were measured every 2 h. Lorentz, polarization, and decay corrections were applied as was an empirical absorption correction based on a series of ψ scans.

Each of the structures was solved by the Patterson method using SHELXS-86 which revealed the positions of the metal atoms. All other non-hydrogen atoms were found by successive difference Fourier syntheses. The expected hydride positions were calculated using the program Hydex[5] and included in the structure factor calculations but not refined in the final least-squares cycles. No other hydrogen atoms were included in the calculations. Final refinement parameters for each crystal are listed in Table I. Selected bond distances and angles are given in Tables III, V, VII, IX, and XI, and fractional atomic coordinates are listed in Tables II, IV, VI, VIII, and X for compounds **2, 9, 12, 13,** and **16**, respectively.

In the case of compounds **2** and **13** an artificial scattering factor which was the mean of carbon and nitrogen scattering factors was used to account for equal populations of disordered carbon and nitrogen atoms bound to the metal in the imidoyl ligand. Unequal populations were tested for compound **13** but did not give as good a fit to the data as equal populations did.

Scattering factors were taken from Cromer and Waber.[30] Anomalous dispersion corrections were those of Cromer.[31] All calculations were carried out on a DEC MicroVAX II computer using the SDP/VAX system of programs.

Acknowledgment. We gratefully acknowledge the National Science Foundation (CHE9016495) for support of this research and for a Chemical Instrumentation Grant (CHE8913125) for purchase of a 360-MHz NMR. We also thank Professor A. Fratiello and R. Perrigan of the California State University, Los Angeles, for help in obtaining 400-MHz ^{1}H NMR data. We also thank the NATO Science Program for a travel grant (E.R. and L.M., 87505).

Supplementary Material Available: Tables 12-16, listing anisotropic displacement factors, and Tables 17-21, listing complete bond distances and angles for **2, 9, 12, 13,** and **16** (24 pages). Ordering information is given on any current masthead page.

OM920748T

(30) Cromer, D. T.; Waber, J. T. *International Tables for X-ray Crystallography*; The Kynoch Press: Birmingham, England, 1974; Vol. IV, Table 2.2B.

(31) Cromer, D. T. *International Tables for X-ray Crystallography*; The Kynoch Press: Birmingham, England, 1974; Vol. IV, Tables 2.3.1.